Flux of Extraterrestrial Materials

Michael Zolensky
NASA Johnson Space Center

Phil Bland
Imperial College

Peter Brown
University of Western Ontario

Ian Halliday
Ottawa, Ontario, Canada

1. INTRODUCTION

In its annual journey around the Sun, Earth continuously experiences collisions with solid objects derived predominantly from asteroidal, cometary, and planetary debris. This debris ranges in size from large objects capable of forming impact craters; down to boulder-sized chunks, some of which deposit meteorites on the ground; to a steady rain of interplanetary and interstellar dust particles. The flux of these materials has been assessed using space-, atmosphere-, and groundbased techniques, and is observed to vary with time to a significant degree. We will describe the resultant flux of extraterrestrial materials in order of decreasing incoming mass, beginning with the current flux of meteorite-producing fireballs.

2. CURRENT METEORITE FLUX FROM FIREBALLS AND GROUND OBSERVATIONS

2.1. Introduction

In this section we consider objects that produce very bright meteors during their atmospheric passage, frequently called "fireballs" or sometimes "bolides" in more technical literature. The faint limit of their brightness is an apparent peak magnitude near –5 (brighter than Venus) with an upper limit of about –15 to –20, limited only by the extreme scarcity of such bright events. This range is suitable for optical detection, traditionally by photography and more recently with various electronic and satellite techniques. The observational data may be used to derive solar-system orbits and, using a knowledge of meteor and atmospheric physics, estimates of mass upon entry into Earth's atmosphere and of any surviving meteorites that reach the ground. For determining flux values, this approach has the obvious advantage that the number of events in a known time interval is rather easily determined. The greatest challenge is to derive valid values for the masses involved. Efforts to determine meteor composition from optical observations have been attempted, with variable success.

Early estimates of the flux of meteorites (on the ground) were based on recovery rates in regions with high population density. It was clear that this method involved large uncertainties, but with the advent of three photographic camera networks in the 1960s and early 1970s, instrumental data gradually became available. These three networks were the European Network in central Europe, with headquarters at the Ondrejov Observatory in the Czech Republic, the Prairie Network in the central plains of the United States, and the Meteorite Observation and Recovery Project (MORP) in the prairie provinces of western Canada. The first flux estimate was for the mass distribution of all objects at the top of the atmosphere (*McCrosky and Ceplecha,* 1969) based on Prairie Network data. The fraction of events related to actual meteorite falls was estimated, indicating a flux 1 to 2 orders of magnitude higher than the previous estimates. This suggested that either the efficiency of meteorite recognition was much lower than expected or there was some problem with the reduction of the camera data.

2.2. Meteorite Observation and Recovery Project Data on Meteorite Masses

One of the goals of the MORP network was to tackle this problem of the flux of meteorites. The network consisted of 12 camera stations providing effective two-station coverage over an area of 1.26×10^6 km^2. The network was in operation from 1971 to 1985 and detailed records of the clear-sky area covered for each night were maintained for 11 years, from 1974 to 1985. A description of the network and details of the techniques used for the flux project were published in several papers (*Halliday et al.,* 1978, 1984, 1989, 1991, 1996). Only a summary of the results is presented here. The total clear-sky coverage in 11 years was

1.51×10^{10} km^2 h. We quote flux values in units of events per 10^6 km^2 per year; the total coverage is equivalent to 1.72 years over 10^6 km^2. Typical search areas in desert regions might be 10 km^2 so the network observed the equivalent infall for nearly 200,000 years for such an area.

Essentially all stony meteorites, and a large proportion of irons and stony irons, fracture during their atmospheric flight. There is convincing evidence that for a relatively small event such as the Innisfree, Canada, fall of 1977, with an estimated entry mass of about 40 kg (*Halliday et al.,* 1981) and for the massive daytime Moravka, Slovakia, event of 2000, whose preatmospheric mass is estimated at 1500 kg (*Borovička and Kalenda,* 2003; *Borovička et al.,* 2003), there was considerable fragmentation above a height of 50 km. At such heights the pressure loading is small enough that fragmentation must be due to preexisting cracks in a meteoroid of low intrinsic strength. Successive fragmentation events at lower heights lead to numerous fragments spread over a strewn field, typically several kilometers in extent, and frequently an order of magnitude larger. It is thus very important to be precise in defining an estimate of flux. Does it refer to the total distribution of all fragments from many events, to the distribution of total masses for each event, to the distribution of the largest fragment from each event, or to the distribution of entry masses at the top of the atmosphere? Attempts may be made to quantify each of these as a flux in some time interval.

Camera networks such as the MORP system are best suited to estimating the mass of the largest fragment for each event. They can also provide estimates of entry masses, although these are less secure. With some assumptions based on favorable meteorite events, the distribution of the largest fragment masses can be converted to the distribution of total masses on the ground.

Two suitable photographs of a fireball can be reduced to give values of height, velocity, and deceleration along the path. Values for deceleration become reliable late in the trail for those meteoroids that penetrate deep into the atmosphere, which are the best candidates for recoverable meteorite falls. The conventional drag equation can then be used to estimate a "dynamic mass" using observed or known values for velocity, deceleration, and atmospheric density, together with reasonable choices for the meteoroid density, drag coefficient, and shape factor, the latter a measure of the ratio of mass to cross-section area. By choosing the lowest portion of the path for which the deceleration is reliable, further ablation or fragmentation is likely not a problem and the dynamic mass obtained should be close to the actual mass of the largest fragment. Normally the largest fragment is the leading one in the cluster of fragments in the trail and the only one for which good decelerations can be derived. In a favorable case, such as Innisfree (*Halliday et al.,* 1981), dynamic masses were obtained for four separate fragments that could be matched to the recovered meteorites on the ground. The agreement between dynamic and recovered masses was quite satisfactory, providing confidence in the values of dynamic masses.

The flux of the largest fragments can be obtained directly from dynamic masses for those objects that are observed under suitable clear-sky conditions. It is, however, more meaningful to estimate the total mass of meteorites from each fall. From consideration of various falls for which recovery is believed to have been reasonably complete, it appears that the largest fragment constitutes a smaller fraction of the total mass as we consider larger events. The most comprehensive examination of this (*Halliday et al.,* 1984, 1989) found an increase from largest fragment to total mass ranged from a factor of 1.25 at 50 g to 4.0 at 20 kg.

Meteorite flux values are usually quoted as cumulative frequencies of the form

$$\log N = A \log m + B$$

where N is the number of events per unit time and area with mass equal to or larger than m. We typically choose N to be the number per 10^6 km^2 per year and express m in grams. (An area of 10^6 km^2 is close to the size of the country of Egypt.)

Figure 1 shows the cumulative distribution for main masses on the ground, shown as M – M and also the estimate for total masses for each event, marked T – T in the figure. There is a marked change in slope near 600 g for the M – M plot, which corresponds to a mass of 1030 g for total masses T – T. This surprising result was considered in some detail by *Halliday et al.* (1989), where it was shown that the deficiency of smaller masses is due entirely to the slower fireballs with initial velocity less than 16 km s^{-1}. The change cannot be due to observational selection effects and is unlikely to be caused by changes in ablation as a function of mass. The most likely cause appears to be a fragmentation effect, although the mechanism is not understood. The T – T plot predicts that nine events per year will de-

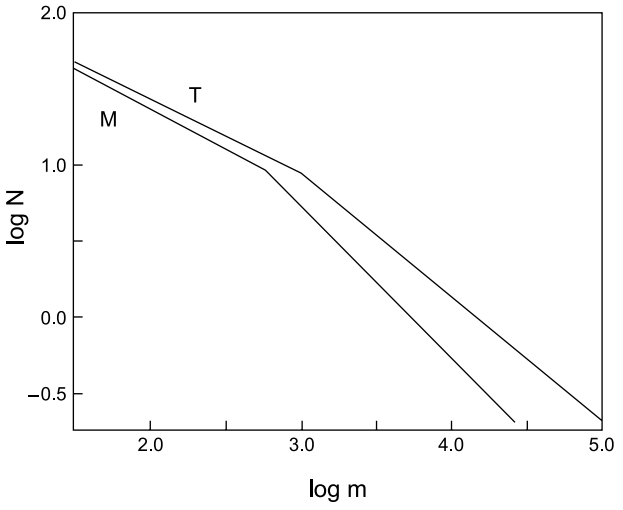

Fig. 1. The cumulative frequencies, N, of number of events per year per 10^6 km^2, as a function of mass, m, in grams, for meteorites on the ground. The line M shows values for the largest fragment of each event while T refers to the total estimated mass for each event.

posit at least 1 kg in an area of 10^6 km^2, while one event in 2 years will deposit 30 kg. The mathematical expressions for Fig. 1 are

for M – M: $\log N = -0.53 \log m + 2.42$ $m < 600$ g
$\log N = -1.00 \log m + 3.72$ $m > 600$ g

for T – T: $\log N = -0.49 \log m + 2.41$ $m < 1030$ g
$\log N = -0.82 \log m + 3.40$ $m > 1030$ g

The nature of the flux problem does not make it appropriate for a formal evaluation of probable errors. Errors in counting the number of events and recording total areas and times of observation are trivial compared to errors in mass calibration. An individual dynamic mass could possibly be in error by a factor of 3 or 4 but it is unlikely that any systematic error greater than a factor of 2 exists in positioning the mass scale in Fig. 1 for the M – M plot. The conversion to total masses on the ground may lead to a somewhat greater uncertainty for the T – T plot.

2.3. Preatmospheric Masses

The MORP observations may also be used to derive the mass influx at the top of the atmosphere. The so-called "photometric masses" are derived from measures of the luminosity along the trail combined with the observed velocity at each point and some knowledge of the "luminous efficiency" with which kinetic energy is converted to luminosity. Much effort has been devoted to the luminous efficiency of meteorites as shown in the discussion by *Ceplecha et al*. (1998). Early estimates of the efficiency were generally considerably less than 1% but values of several percent have been adopted more recently. Some authors have used a simple dependence of the efficiency with velocity and, of course, the values should depend on the wavelength used in a particular set of observations. The MORP reductions used a constant value of 0.04 for the panchromatic wavelength band of the film in use. *Borovička et al.* (2003) determined a value of 0.09 for the larger bolometric range for the Moravka meteorite event. Considerable mass loss may occur during brief flares along a fireball's path where a sudden fragmentation event produces a cloud of small particles that then ablate very rapidly. For the Moravka event, *Borovička and Kalenda* (2003) state that such events were the major mass-loss process. It is thus important to measure the brightness of these flares to determine the mass loss. Moravka, with an initial velocity of 22.5 km s^{-1}, is among the fastest group of meteorite events, so the importance of fragmentation here may also have been greater than normal.

The MORP clear-sky survey observed 754 fireballs from which an unbiased sample of 213 events was studied in detail, and photometric mass estimates were published for each of these (*Halliday et al.,* 1996). This group includes fragile cometary material such as bright members of numerous annual meteor showers. (All potential meteorite events were studied, including those observed under poor sky conditions, but the group of 213 represents a typical sample of bright meteoroids.) This data can be divided into several subgroups. One group of predominantly asteroidal origin was defined by initial velocity less than 25 km s^{-1} and nonmembership in a known meteor shower, while the faster objects and all shower members were called the "cometary" group. From the physical data, primarily density estimates for the meteoroids, it appears that perhaps one-fourth of both groups are misplaced in the wrong group by this rather arbitrary division.

Figure 2 shows some of the mass distributions at the top of the atmosphere. The line A – A represents the total influx of fireballs, B – B the "asteroidal" group defined above, C – C the "cometary" group, and D – D those objects that survive to drop meteorites. For an initial mass of 10 kg our result is a factor of 10 below the early Prairie Network value (*McCrosky and Ceplecha,* 1969), due mainly to the low value for luminous efficiency in use at that time. For entry masses of a few kilograms it appears there are roughly two objects of asteroidal origin for every cometary object. The asteroidal plot B – B has a steeper slope for masses larger than about 2.7 kg, which is also seen in the A – A plot for all objects since asteroidal meteoroids dominate the entire group.

The mathematical expressions for the plots of Fig. 2 are listed below, together with the approximate mass range for each expression.

All objects:
A – A $\log N = -1.06 \log m + 5.26$ 2.4 to 12 kg
A – A $\log N = -0.48 \log m + 3.50$ 0.1 to 2.4 kg

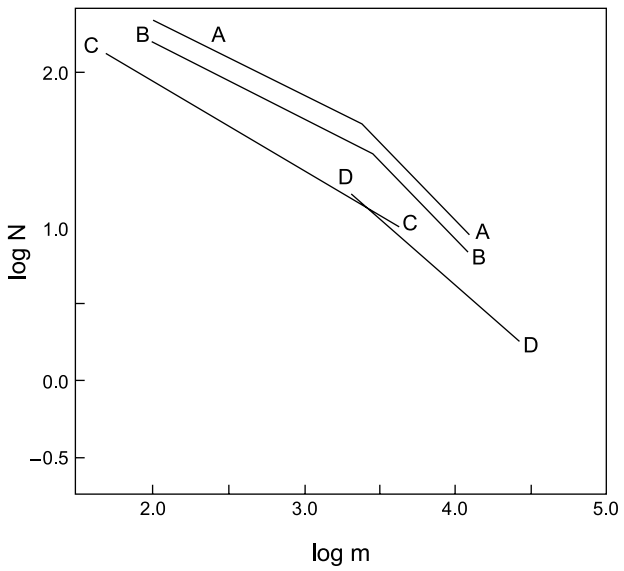

Fig. 2. Cumulative frequencies as in Fig. 1 for preatmospheric masses. A = the total influx of all meteoroids; B = the influx of asteroidal material; C = the influx of cometary meteoroids; D = those objects that deposit meteorites of at least 50 g on the ground.

Asteroidal:
B – B log N = –1.00 log m + 4.92 2.7 to 12 kg
B – B log N = –0.50 log m + 3.20 0.1 to 2.7 kg

Cometary:
C – C log N = –0.60 log m + 3.15 0.05 to 4 kg

Meteorite:
D – D log N = –0.87 log m + 4.09 2.0 to 25 kg

Photometric masses are generally less secure than dynamic masses due to problems in calibrating the luminosity scale, especially for very bright events, and the appropriate value for luminous efficiency is also in some doubt. One might have used a higher value for the efficiency in the MORP reductions, which would lower the mass estimates. We can examine the fraction of the initial mass that survives as meteorites for meteorite events by comparing the preatmospheric mass and the estimate for total masses on the ground. There is a large range in the survival fraction due primarily to velocity differences, but equally important are the slope of the atmospheric path and the severity of fragmentation. The median value for the survival from the MORP data is 0.20, a reasonable value that lends some confidence to the photometric masses.

For comparison, *Ceplecha* (2001) adopts a different value and functional dependence for luminous efficiency than *Halliday et al.* (1996) and makes use of Prairie Network and European Network data for large fireballs and finds a flux ~2× higher than Halliday et al. over the mass interval from 10 g–10 kg (Fig. 3). The physical makeup of these bodies appears to be roughly 50% cometary and 50% asteroidal. Halliday et al. finds that 50–70% of all fireballs in this mass range are asteroidal in physical strength (with the proportion becoming higher as the mass increases), while *Ceplecha* (1994) finds 45–60% are asteroidal over the observed size range from 0.1–1 m, with asteroidal bodies again increasing as mass increases. Here we take asteroidal bodies to be type I and II fireballs in the scheme of *Ceplecha et al*. (1998), which are assumed to correspond to ordinary and carbonaceous chondrites respectively. *Ceplecha* (1994) also estimates that the proportion of cometary-type bodies begins increasing again above 1 m in diameter; however, this is largely an extrapolated result with little constraining observational data. Based on the recent work of *Brown et al*. (2002a) and its agreement with *ReVelle* (1997), it seems probable that the trend toward increasing proportions of solid (asteroidal) bodies continues to much larger sizes (>10 m). Indeed, the best current telescopic estimates from dynamical arguments and spectral measurements have the fraction of the near-Earth asteroid (NEA) population, which might be extinct cometary nuclei, as 10–18% (*Binzel et al.,* 2004), basically consistent with this result (cf. *Weissman et al.,* 2002).

Camera networks provide influx rates for at most a few decades, while collections of meteorites from hot deserts and Antarctica should represent an average over many thousands of years. We have good agreement between the camera results and the analysis of desert meteorite collections, while spacecraft and infrasonic observations extend the coverage to both larger and smaller mass ranges.

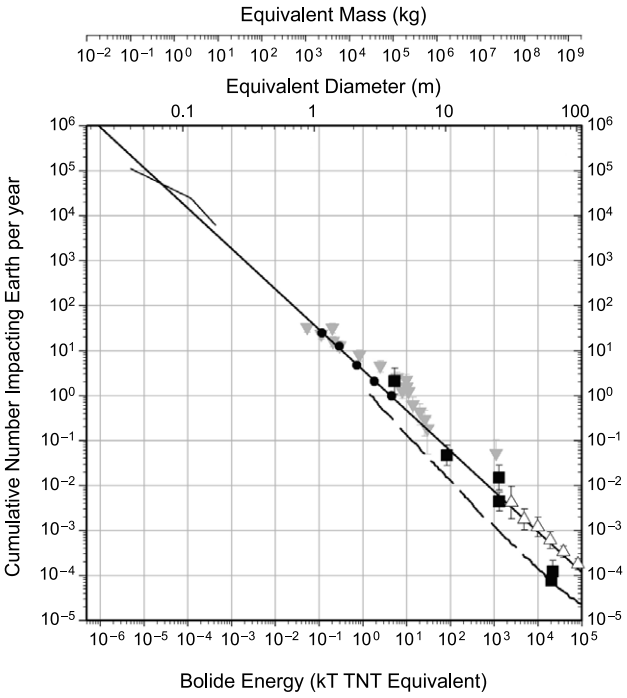

Fig. 3. Fluxes for meteoroids in the 0.01–100-m size range. Data are from groundbased camera observations of bright meteors/fireballs (*Halliday et al.,* 1996) (thin solid line), satellite fireball data (*Brown et al.,* 2002a) (filled circles), infrasound measurements (*ReVelle,* 1997) (gray inverted triangles), telescopic observations [*Rabinowitz et al*. (2000), from Spacewatch data, solid black squares; *Harris* (2002), from LINEAR data, open triangles], and estimates from lunar cratering [*Werner et al.* (2002), lower dashed line]. All flux curves are computed assuming a mass weighted average impact velocity of 20.3 km/s. Diameters are computed assuming bulk densities of 3 g cm^{-3}. The solid line running through the figure is the power law $N = 3.7E^{-0.90}$ fit to the satellite fireball data of *Brown et al.* (2002a). 1 kt TNT equivalent = 4.185×10^{12} J.

2.4. Satellite and Infrasound Observations

Satellite observations of meteoroids entering Earth's atmosphere began with the spectacular August 10, 1972, Earth-grazing fireball over the western portion of North America (*Rawcliffe et al.,* 1974). *Tagliaferri et al.* (1994) summarize the basic properties of the spacebased sensors involved in gathering these data. Regular, automated detection of fireballs with these spacebased sensors began in 1994 and continues to the present time. These sensors detect ~meter-sized and larger bodies impacting Earth, al-

though the actual data measured is integrated optical brightness for a particular fireball in the silicon passband (cf. *Brown et al.,* 1996). To generate meaningful flux values from these optical energies, the conversion efficiency of initial kinetic energy of the body to light in the passband of the sensor is needed, as is an assumed entry velocity. The calibration of this satellite luminous efficiency has been attempted by *Brown et al.* (2002a). They make use of satellite fireball events detected with other instruments or by comparison of satellite energies with events having recovered meteorites to constrain the initial meteoroid size. Implicit in all these determinations is the assumption that fireball radiation follows a 6000 K blackbody; this is at best a gross approximation and at worse incorrect (cf. *Jenniskens et al.,* 2000). Nevertheless, *Brown et al.* (2002a) were able to derive an empirical fit to the luminous efficiency that matched theoretical predictions well (*Nemtchinov et al.,* 1997) and produced flux values compatible with telescopic observations of 10-m+-sized bodies (cf. *Rabinowitz et al.,* 2000). An updated version of their calibration curve is shown in Fig. 4 along with a comparison to theoretical values computed by *Nemtchinov et al* (1997). Using these calibration values for the luminous efficiency, the satellite-determined cumulative annual global flux of meteoroids with energy E (in kilotons of TNT equivalent energy = 4.185×10^{12} J) was found to be $N = (3.70 \pm 0.13)E^{-0.90 \pm 0.03}$ valid in the energy interval from $0.1 < E < 20$ kt. Assuming a mean impact velocity with Earth of 20.3 km s^{-1}, these bodies range in size from 1–7 m in diameter.

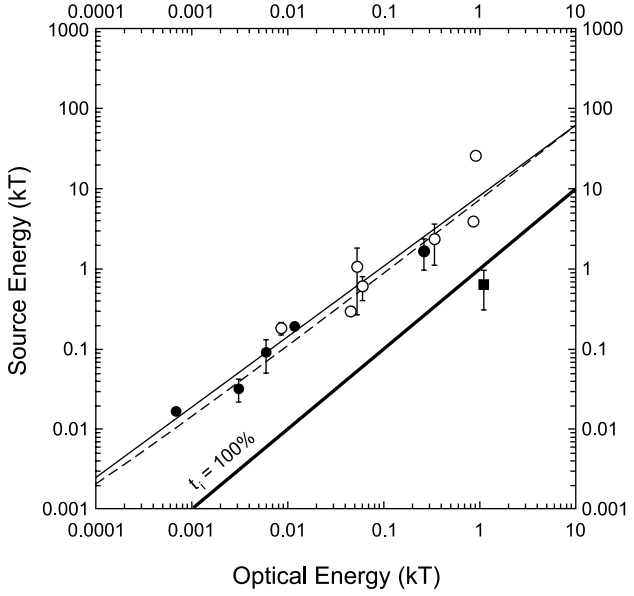

Fig. 4. An empirical fit to the integral luminous efficiency for meter-sized impactors detected by spacebased sensors. The empirical fit (thin solid line) to integral luminous efficiency in this figure is used to compute the total energy (and through an assumed velocity impacting mass) for bolides in the 0.1–10-m range. The filled circles represent individual bolide events that have energy estimates of highest reliability based on groundtruth data (meteorite recoveries, photographic or video data), while open circles are events that have energy measurements based on acoustic data only [following the technique described in *ReVelle* (1997)]. The dashed line is the theoretical integral luminous efficiency expected for bodies with H-chondrite composition (*Nemtchinov et al.,* 1997). The area below the thick solid line shows the region where more than 100% of the initial energy would be required to match the optical brightness, hence this region is unphysical.

Other flux measurements in this size range are available from infrasound records of bolide airbursts (*ReVelle,* 1997), from a small number of NEA observations (*Rabinowitz et al.,* 2000), and from extrapolation of small lunar cratering events (*Werner et al.,* 2002). Werner et al. found an impact rate on Earth for objects >4 m of 0.9 ± 0.1 per year from the lunar cratering record. In contrast, *Rabinowitz et al.* (2000), based on two NEA detections by the Spacewatch telescope, normalized the Spacewatch size-frequency distribution to the calibrated NEAT flux and found a cumulative impact rate of 2.1 ± 1.1 objects >4 m in diameter per year globally. The discrepancy between the lunar result and data based on telescopic observations is likely not significant considering the uncertainties. For example, the lunar flux values represent long-term averages; if the present impactor flux is slightly elevated, this could easily account for the factor of 2–3 disparity. *ReVelle* (1997), based on some 21 infrasonically detected bolide airwave events, derives a value of 2.5 ± 0.8 to the same equivalent energy/size per year globally. The largest single event in the infrasonic record reported by ReVelle is a 1.1-Mt-equivalent fireball that occurred over the South Atlantic on August 3, 1963. If the yield for this event is accurate, it implies an influx rate of 0.05 ± 0.05 objects globally per year >25 m diameter, a value that is much larger than either the *Rabinowitz et al.* (2000) value of $4 \times 10^{-3} \pm 3 \times 10^{-3}$ or the *Werner et al.* (2002) value of 6×10^{-3} for the same size. The small number statistics, combined with uncertainties in the albedo for such small asteroidal bodies (cf. *Binzel et al.,* 2002), means that the flux of bodies in the 10–30-m size range to Earth is the most uncertain portion of the size-frequency spectrum. More recently, *Harris* (2002) has derived impact rates from LINEAR data for objects with diameters >30 m. His results are comparable (within error) to more recent values, also from the LINEAR survey (*Stuart and Harris,* 2004), and represent a first step in filling in the uncertainties in this size range (see Fig. 3 for a summary).

3. METEORITE FLUX ESTIMATES FOR THE PAST BASED ON METEORITE RECOVERY RATES

3.1. Introduction

Initial attempts to determine the flux of meteorites in the mass range $10–10^6$ g used data on the recovery of eyewit-

nessed falls in densely populated areas (*Brown,* 1960, 1961; *Hawkins,* 1960; *Millard,* 1963; *Buchwald,* 1975; *Hughes,* 1980). Unfortunately, estimates of flux calculated using this technique have varied by more than 4 orders of magnitude, probably as a result of the difficulty of unambiguously constraining a number of parameters inherent in this method, e.g., population density, season, time of day, etc. As described above, direct observations of fireballs using camera networks have provided an estimate of the present flux of meteorites and its mass distribution. In particular, data from the Canadian MORP camera network (*Halliday et al.,* 1989) suggest a present flux of 83 events of mass equal to or greater than 1 g per 10^6 km^2 per year. This estimate is well constrained, but there is an uncertainty in deriving a dynamical mass from a fireball image, since at the time of the study only three imaged meteorites had been recovered to provide a comparison. This uncertainty gave rise to an approximate factor of 2 error in the MORP data (*Halliday et al.,* 1991).

Given that only one well-constrained dataset exists, and considering that flux in the meteorite size range helps to constrain the wide range of estimates for the rate at which small crater-forming events occur on Earth, an independent estimate of flux in the meteorite size range is valuable.

Another method for calculating meteorite flux, and more importantly, potential temporal variations in flux, involves analyses of meteorite accumulation sites. There are several locations on Earth where, due to favorable conditions, meteorites accumulate in large numbers. Among these are numerous hot desert sites, including the Sahara, Arabian Peninsula, Roosevelt County, New Mexico, and the Nullarbor Region of Australia, and the cold desert of Antarctica (*Annexstad et al.,* 1995). Meteorites survive for long periods in these areas because moisture level and weathering rates are low, and they are frequently recognized because of a contrast between "dark" meteorites and "pale" country rock or ice. In theory, these accumulation sites should record the integrated flux throughout the meteorite mass range over the lifetime of the accumulation surface.

Aside from offering an independent means of confirming the present flux, this method also offers the intriguing possibility of observing changes in flux over time. This would potentially elucidate meteoroid delivery mechanisms, the operation of meteoroid streams, and the compositional nature of the main asteroid belt. For example, there is compelling evidence that some portion of the meteoroid complex is in the form of short-lived (10^4–10^5 yr) co-orbital streams (*Jopek et al.,* 2002; *Gladman and Pauls,* 2005), such as groups of asteroid families with similar orbits (*Drummond,* 1991; *Rabinowitz et al.,* 1993), identical fall times of meteorites with similar orbits (*Halliday,* 1987), and differences between "old" Antarctic meteorite populations and more recent falls (*Dennison et al.,* 1986). Some claims for identification of meteorites resulting from streams remain controversial, since the cosmic-ray-exposure histories of some of these meteorites span a large spectrum of ages (*Schultz and Weber,* 1996), while calculations indicate that co-orbital streams would not be stable over the excessive timescales required (*Wetherill,* 1986; *Jopek et al.,* 2002; *Gladman and Pauls,* 2005). Analyses of meteorite populations and modeling their flux (by constraining weathering rates) may help in resolving this controversy.

Finally, although we can derive the flux of small (less than a few kilograms) meteorites from camera network data or analysis of meteorite accumulations on Earth, neither approach is effective in estimating the impact rate of larger (~10–10^5 kg) meteorites. The number of fireball events of this size is too low, and the number of desert finds too small, to allow an accurate estimate. However, as we noted above, there are data for the flux of large meteoroids at the top of Earth's atmosphere. If we can model the effects of the atmosphere on a given bolide, and we perform that modeling for a large number of cases over a large enough mass range, then it should be possible to extrapolate the upper atmosphere flux to a flux at Earth's surface. *Bland and Artemieva* (2003) took this approach to constrain the impact rate of objects from 10^2 to 10^{12} kg at Earth's surface.

Given knowledge of meteorite pairing, weathering, and removal and recovery rates it should be possible to discern changes in flux and mass distribution with time (hot deserts retain meteorites for up to at least 10^5 yr, while meteorites may survive in Antarctica for more than 10^6 yr). The idea behind this approach is that if the number of meteorite samples per unit area on the ground today is known, and the rate at which they are removed by weathering (characterized by a so-called "decay constant," λ) is calculated, then ideally we can work back to derive an estimate of the number that fell to Earth initially. However, several difficult problems with this approach must first be addressed: (1) An accurate age for either the accumulation surface and/or terrestrial ages for the meteorite population is required. (2) The action of chemical and physical weathering in removing samples must be quantified and, in any case, be minimal. (3) No other process can have acted to remove samples, e.g., no streams. Ideally, meteorites must be buried for the majority of their terrestrial history, and only recently have been excavated. (4) All the meteorite samples within a known catchment area are recovered and a study to pair samples successfully undertaken, so that a "population density" of meteorites per unit area is known. (5) The search area is large compared to the typical strewn field size. Failure to take this factor into account may mean that an area samples an unrepresentative number of falls (see *Halliday et al.,* 1991). We discuss aspects of these factors below.

3.2. Weathering Rate

Accurately modeling the weathering decay rate of meteorite samples has significance principally for two reasons. First, it allows us to quantify part of the interaction between Earth-surface environments and rock weathering. Second, in hot deserts, weathering (chemical and mechanical) is likely to be the sole means by which meteorite samples are removed from a population. As such, given a well-constrained decay rate and a measure of the number of meteorites per unit area, it is possible to make an accurate estimate of the

flux of meteorites to Earth over the accumulation period. Terrestrial weathering is covered in detail in *Bland et al.* (2006).

3.3. Terrestrial Ages

In order to quantify the weathering decay rate for meteorites, it is necessary to establish an absolute chronology. Fortunately, this is possible based on the measured exposure times of the meteorites since landing on Earth, known as the terrestrial age. Over the last 30 years a variety of methods have been used to determine the terrestrial ages of meteorite finds, most of which analyze the abundance of cosmogenic radionuclides produced while the meteorite is in space. In almost all cases, the time it takes for a sample to migrate from the asteroid belt to an eventual impact with Earth (its cosmic-ray-exposure age) is significantly greater than the time needed for a saturation level of the appropriate cosmogenic radionuclides to build up in the meteorite. After the sample lands on Earth, it is largely shielded from cosmic rays and the abundance of cosmogenic radionuclides declines from a saturation level as the unstable isotopes decay. Depending on their period of terrestrial residence, the decay of several cosmogenically produced radionuclides, such as ^{14}C (halflife 5730 yr), ^{81}Kr (halflife 210,000 yr), ^{36}Cl (halflife 301,000 yr), and ^{26}Al (halflife 740,000 yr), have been used to determine the terrestrial ages of meteorites (e.g., *Honda and Arnold,* 1964; *Chang and Wänke,* 1969; *Fireman,* 1983; *Jull et al.,* 1990; *Nishiizumi,* 1990; *Nishiizumi et al.,* 1989a; *Freundel et al.,* 1986; *Aylmer et al.,* 1988; *Scherer et al.,* 1987; *Welten et al.,* 1997). These workers have reported terrestrial ages for Antarctic meteorites ranging up to ~3 m.y. For stony meteorites from the world's "hot" desert regions that have been dated so far, *Jull et al*. (1993a,b, 1995) and *Wlotzka et al*. (1995a,b) have reported ^{14}C ages >40,000 yr. The ^{14}C-dating technique measures the decay of cosmogenic radiocarbon produced in space and separates ^{14}C produced by cosmic-ray bombardment from ^{14}C accumulated by the meteorite from terrestrial sources such as organic contamination and weathering. The main source of error in this analysis comes from the possibility that some level of shielding occurred if the meteorite was buried at some depth on a large meteoroid while in space. Consideration of this (e.g., *Jull et al.,* 1995) gives rise to much of the comparatively large (~1300 yr) error on an individual ^{14}C terrestrial age.

One means of estimating decay rates for hot desert (*Zolensky et al.,* 1992) and Antarctic (*Freundel et al*., 1986) meteorite populations has been to use terrestrial ages plotted as a frequency distribution. In a complete population for which reliable pairing data are available, an exponential decrease in frequency over time is expected. The slope of the distribution approximates to a weathering decay rate. This approach is effective provided the terrestrial age dataset is large enough to enable the slope to be well constrained; however, for most populations either sufficient samples are not available or the terrestrial-age dataset is not yet large enough. As described in *Bland et al.* (2006), one can constrain the effect of weathering in actually removing samples from a population. This, combined with the weathering rate, allows an estimate of the decay constant λ to be made (see *Bland et al.,* 1996a,b).

3.4. Number and Mass of Meteorites Arriving on Earth

To obtain an estimate of flux for each desert accumulation site, calculated values for λ are related to the density of paired meteorites over a given mass per unit area. For example, for Roosevelt County meteorites, λ is 0.032 k.y.$^{-1}$, and the density of meteorites per km^2 over 10 g in mass is 39/10.8 (39 meteorites >10 g found in an area of 10.8 km^2), which is 3.6. Given these data, the flux calculation for meteorites over 10 g in mass per 10^6 km^{-2} yr^{-1} is $0.032 \times 3.6 \times 1000$, which yields an estimate of 115 events. This estimate can be extrapolated to larger masses by using the slope of the mass distribution for each site. Generally a power law is chosen for the flux rate of the form $N_o(M) = cM^A$. A is the slope of the mass distribution and has different values over different mass ranges (*Halliday et al.,* 1989). MORP camera network data indicate a value of –0.49 for the mass range ~0.01–1 kg. The mass distribution may also be derived from an analysis of paired sample populations in accumulation sites. *Zolensky et al*. (1990, 1992) found a value of –0.54 for the Roosevelt County population, so to extrapolate to events over 500 g from the initial 10 g one takes $50^{-0.54} \times 115$, which is approximately 14. In this manner, given data on the local decay constant, mass, and aerial distribution for each site, a meteorite flux can be calculated for approximately the 10 g–1 kg mass range. Taking a similar approach for the Nullarbor Region yields 36 meteorites over 10 g in mass per 10^6 km^{-2} yr^{-1}, and for the Sahara, 95 meteorites over 10 g in mass per 10^6 km^2 yr^{-1}. Averaging the three sites, the meteorite accumulation site method yields an estimate of 82 meteorites over 10 g in mass per 10^6 km^2 yr^{-1}, remarkably close to the *Halliday et al.* (1989) estimate of 83 meteorites. Thus there is good agreement between the meteorite flux as calculated from camera networks and desert recovery sites. Given that the surface area of Earth is 5.11×10^8 km^2, these results would suggest ~42,000 meteorites >10 g in mass arriving at Earth per year (or more than 100 per day).

Bland et al. (1996a) also arrived at an independent estimate of the total amount of material in the meteorite size range that arrives at Earth's surface, by integrating over the mass range of interest. *Halliday et al*. (1989) (equations (6) and (7)) give

$$\log N = \begin{cases} 2.41 - (0.49) \log m_T & \text{for } m_T \le 1030 \text{ g} \\ 3.40 - (0.82) \log m_T & \text{for } m_T \ge 1030 \text{ g} \end{cases}$$

so

$$\log N(m_T) = \begin{cases} 2.41 - (0.49) \log m_T & \text{for } m_T \le 1030 \text{ g} \\ 3.40 - (0.82) \log m_T & \text{for } m_T \ge 1030 \text{ g} \end{cases}$$

where N is the number of mass $\ge m_T$ grams per 10^6 km^2 yr^{-1}.

Bland et al. (1996a,b) derive a similar relationship for a number of hot desert accumulation sites for masses <1 kg

$\log N = 2.13 - (0.58) \log m_T$ for the NR
$\log N = 2.60 - (0.54) \log m_T$ for RC
$\log N = 2.65 - (0.67) \log m_T$ for the SD ($R^* = 0.46$)
$\log N = 3.31 - (0.67) \log m_T$ for the SD ($R^* = 0.32$)

If N(m) is equal to the number per 10^6 km^2 yr^{-1} of mass greater than m, then the number per 10^6 km^2 yr^{-1} lying between m and m + dm is

$$N(m) - N(m + dm) = -\frac{dN(m)}{dm} dm$$

So the mass on the ground (per 10^6 km^2 yr^{-1}) between m and m + dm is

$$-m\frac{dN(m)}{dm} dm$$

From *Halliday et al.* (1989) we can write

$$N(m) = \begin{cases} c_1 m^{A_1} \text{ for } m \le 1030 \text{ g}; c_1 = 10^{2.41}, A_1 = -0.49 \\ c_2 m^{A_2} \text{ for } m \ge 1030 \text{ g}; c_2 = 10^{3.40}, A_2 = -0.82 \end{cases}$$

This gives

$$-m\frac{dN}{dm} = \begin{cases} -A_1 c_1 m^{A_1} \text{ for } m \le 1030 \text{ g} \\ -A_2 c_2 m^{A_2} \text{ for } m \ge 1030 \text{ g} \end{cases}$$

Considering all masses between m_L and m_U (where m_L = 1030 g and m_U = 1030 g) then the total mass per 10^6 km^2 yr^{-1} is

$$M = \int_{m_L}^{1030} -A_1 c_1 m^{A_1} dm + \int_{1030}^{m_U} -A_2 c_2 m^{A_2} dm$$

$$= -\left(\frac{A_1 c_1}{A_1 + 1}\right)\left[(1030)^{A_1 + 1} - (m_L)^{A_1 + 1}\right]$$

$$-\left(\frac{A_2 c_2}{A_2 + 1}\right)\left[(m_U)^{A_2 + 1} - (1030)^{A_2 + 1}\right]$$

Taking the above values for A_1, c_1, A_2, and c_2 from *Halliday et al.* (1989), between m_L = 10 g and $m_U = 10^6$g, *Bland et al.* (1996a) find M = 105.3 kg per 10^6 km^2 yr^{-1}. Given that the surface area of Earth is 5.11 ×10^8 km^2, this analysis suggests a total mass flux to Earth in the meteorite size range of 5.38 × 10^4 kg yr^{-1}, consistent with earlier estimates.

3.5. The Flux of Large Meteorites at Earth's Surface

Given the flux of large meteoroids at the top of Earth's atmosphere, and a well-constrained model of the effect of the atmosphere on a given bolide, it is possible to extrapolate the upper atmosphere flux to a flux at Earth's surface. *Bland and Artemieva* (2003) used this method to constrain the impact rate of bodies <1 km diameter at Earth's surface. Although there are gaps in the upper atmosphere data, *Bland and Artemieva* (2003) showed that overall shape of the size-frequency distribution (SFD) is similar to that calculated for impactors on the Moon and Mars, and to the observed population of near-Earth objects (NEOs) and main-belt asteroids. Thus, constraining one portion of the SFD constrains the rest. Based on this calculated SFD for the upper atmosphere, and using a model that calculates motion, aerodynamic loading, and ablation for each individual particle in a fragmented impactor, they were able to extrapolate the upper atmosphere impactor SFD to an impactor SFD for Earth's surface. The so-called "separated fragments" (SF) model allowed them to calculate fragmentation and ablation in Earth's atmosphere for a range of impactor types and masses. The SFD that *Bland and Artemieva* (2003) derived for Earth's surface suggests that a 1-t meteoritic mass arrives on Earth approximately once a year, a 10-t mass every 15 years, and a 100-t mass every 200 years. Their modeling further suggests that >95% of these bodies will be irons.

3.6. Meteorite Flux and Populations Based on Antarctic Finds: A Window into the Meteorite Flux over the Past 3 Million Years

Since preservation and recovery factors are best attained in Antarctica, as shown by 30 difficult years of collection activity, we discuss work on these meteorites as a special case. Meteorite recovery expeditions over the past 30 years by the National Institute of Polar Research, National Science Foundation, and EUROMET have returned more than 30,000 meteorite specimens from Antarctica, probably representing more than 2000 individual falls (*Annexstad et al.,* 1995). The population of recovered Antarctic meteorites thus outnumbers the entire harvest from falls over the remainder of Earth that has collected over the past 13 centuries (some very old falls have been preserved in Japan). Terrestrial age determinations have revealed that meteorites have been preserved for up to 3,000,000 years in Antarctica, although most have a terrestrial residence time of less than 100,000 years (*Nishiizumi et al.,* 1989a; *Nishiizumi,* 1995; *Welten,* 1995; *Scherer et al.,* 1987). Elsewhere on Earth meteorites are generally completely weathered away in 10^4–10^5 yr. The population of Antarctic meteorites contains numerous types not found (or rarely so) elsewhere on Earth, such as lunar meteorites, certain irons, and metamorphosed carbonaceous chondrites. Some workers report compositional variations in the H chondrites with time. These various reports suggest changes in the source asteroids feeding material to Earth over the past several hundred thousand years (*Michlovich et al.,* 1995). However, many of these unusual meteorites are small in mass, and therefore are most easily located on a white, rock-free environment, leading one to speculate that a collection bias is at work (*Huss,* 1991). It is thus desirable to reexamine how the population of meteorites to Antarctica through the ages compares to the mod-

ern record. Here we will explain the barriers to this goal and progress that is being made.

According to the general model, as meteorites fall from space onto the Antarctic plateau, they get incorporated into a growing pile of snow and ice within a few years (*Whillans and Cassidy,* 1983, *Cassidy et al.,* 1992; *Delisle and Sievers,* 1991). From this time until they emerge somewhere downslope they are locked into cold ice, subject only to very slow weathering [by the action of "unfrozen water" (see *Zolensky and Paces,* 1986)] and some dynamic stress as the ice flows toward the periphery of the continent, where it drops into the ocean. However, in some areas the ice has to pass over or around major mountain ranges (often buried but still felt by the ice), and in these areas the ice has to slow down, increasing exposure of the ice to the dry katabatic winds and causing increased sublimation. Over thousands of years meteorites can be highly concentrated at the surface on temporarily stranded, dense, blue ice. In some situations (e.g., the Pecora Escarpment) meteorite stranding zones are not directly downflow of glaciers, but rather appear to have moved laterally for poorly understood reasons, in a sort of "end run" around the front of an obstruction (J. Schutt, personal communication, 1991). These stranding surfaces appear to be stable until increased snowfall upslope increases the flow of ice downslope, flushing the meteorites away. It is possible for one stranding surface to form and be flushed downstream only to reemerge later. Each stranding surface contains at least two populations of meteorites. The first are those that traveled in the ice to the stranding site, and therefore represent a snapshot of the meteorite flux from the past (older meteorites have been flushed away, younger ones are upstream still entrained in the ice). The second population is provided by recent direct falls onto the stranding surface. The presence of at least two chronologically distinct meteorite populations considerably complicates any calculation of meteorite flux based upon statistical considerations. In fact, *Huss* (1990a,b) has argued that nearly all meteorites in stranding surfaces fell directly there, that the stranding surface is not in fact moving significantly, and that the accumulation times calculated from the terrestrial ages of the meteorites can therefore be used to date the period over which the ice has been stalled. This model is based upon a careful consideration of the meteorite mass/number populations. The conflicts between Huss' model and that by *Cassidy et al.* (1992) have not been resolved. This is obviously a major impediment to the use of meteorite populations to calculate meteorite flux; nevertheless, we move bravely onward.

3.7. Calculation of Antarctic Meteorite Flux

There are numerous uncertainties that currently impede calculation of meteorite flux from Antarctic collections, most of which cannot be easily circumvented (*Harvey and Cassidy,* 1991). We review these factors below.

3.7.1. Terrestrial age dating of meteorites. In terrestrial age determinations of Antarctic meteorites (principally chondrites) the isotopes ^{36}Cl, ^{81}Kr, ^{10}Be, ^{14}C, and ^{26}Al are most effectively employed (*Nishiizumi et al.,* 1989a; *Wieler et al.,* 1995; *Welten,* 1995). There is a measurement gap between ^{14}C ages (<40 ka) and ^{36}Cl ages (>70 ka). *Nishiizumi* (1995) has suggested that this gap might be closed by future investigations of cosmogenic ^{41}Ca. Unfortunately, it is not currently easy to measure ^{41}Ca in chondrites.

Due principally to the sheer bulk of recovered meteorites, available funding, and finite lifetimes of meteorite investigators, only about 1% of the Antarctic meteorites have had their terrestrial ages determined (*Nishiizumi et al.,* 1989a; *Nishiizumi,* 1995; *Wieler et al.,* 1995; *Welten,* 1995); these are principally by ^{36}Cl. Indirect means must be found to date the remainder.

Benoit, Sears, and coworkers have suggested that natural thermoluminescence (TL) can be used to help address this problem in the interim (*Benoit et al.,* 1992, 1993, 1994). In this technique, one assumes a mean annual temperature for the storage of Antarctic meteorites and a "surface exposure age" as part of the terrestrial age is deduced. According to these TL measurements most of the meteorites spend <50% of their terrestrial history on the surface of the ice in Antarctica, with this conclusion being based upon their low relative TL sensitivity, which in turn is related to their degree of postexposure weathering. While this technique cannot be used to obtain absolute terrestrial ages, the calculated exposure ages could be of value in comparing the histories of the different Antarctic stranding surfaces. However, we note that *Welten et al*. (1995) have sounded a dissenting note on the applicability of TL to this problem.

We show results for approximately 280 dated chondrites in Fig. 5 [data from *Nishiizumi et al.* (1989b), *Wieler et al.* (1995), *Welten* (1995), and *Michlovich et al.* (1995)]; the complex nature of meteorite preservation is well displayed.

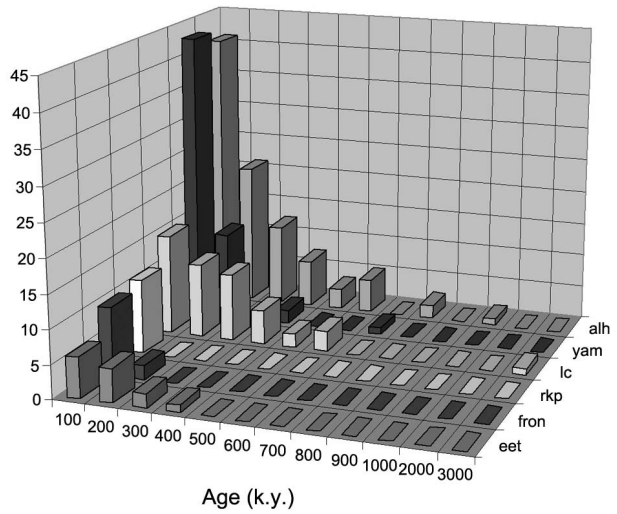

Fig. 5. Distributions of terrestrial ages of meteorites from diverse locations in Antarctica. Alh = Allan Hills, yam = Yamato Mountains, lc = Lewis Cliff, rkp = Reckling Peak, fron = Frontier Mountains, eet = Elephant Moraine.

The Antarctic meteorites display terrestrial ages ranging up to 3 Ma, although chondritic terrestrial ages from different Antarctic ice fields have different distributions. The oldest meteorites are generally found at the main ice field of Allan Hills and Lewis Cliff. In particular, the Lewis Cliff ice field appears to have the best record of meteorites, since the decay of its meteorite population with terrestrial age is least pronounced (Fig. 5). The Lewis Cliff ice tongue appears to be the oldest of the investigated ice field stranding areas (*Welten,* 1995; *Welten et al.,* 1995). At the other end of the scale, terrestrial ages of chondrites recovered from Frontier Mountain are <140 ka, indicating that this is a relatively recent stranding surface.

Various schemes have been proposed for the estimation of terrestrial ages for entire stranding surface meteorite populations. For a given stranding surface one could assume that all meteorites are younger than the oldest measured meteorite, and that meteorite recovery is 100%, but this is certainly not the case, as explained below. Workers have also attempted to characterize the accumulation age of stranding surfaces by examining the mass distributions and weathering lifetimes of meteorites (*Huss,* 1990b). Finally, it would appear that merely measuring the age of a particular blue ice stranding surface and counting up the meteorites presented there would permit the measurement of the flux rate of meteorites to that surface, but we have shown above that at least two distinct meteorite populations are always present. Nevertheless, of all factors to be considered in the derivation of past meteorite flux for Antarctica, terrestrial age is one of the best constrained.

3.7.2. Uncertain meteorite catchment area. In other regions of Earth you can easily measure the area you are searching for meteorites, enabling a flux per unit area to be calculated. This is not directly possible in Antarctica because the meteorites exposed today at a stranding surface have fallen over a far larger glacial tributary system. This situation is further complicated by the fact that the ice movement is irregular, and velocity is not constant. Tributary ice streams can provide additional meteorites with an irregular periodicity. G. Delisle (*Delisle and Sievers,* 1991; *Delisle,* 1993, 1995) has shown that glacial stages result in thicker coastal ice, while interglacials produce thinner coastal ice. The consequences of this are seen in a change of velocity and mass transport of ice with the entrained meteorites. The meteorites at Allan Hills and possibly Frontier Mountain are suspected to have been buried and reemerged, as the interglacial sublimation rates are much higher than the glacial sublimation rates. In this picture the meteorite traps are not stagnant regions, but are continually readjusting to the pattern of glacial and interglacial periods. The uncertain nature of the meteorite catchment area appears to be a severe impediment to the successful calculation of meteorite flux from Antarctic data.

3.7.3. Paleo-stranding surfaces. During periods of increased snowfall upstream, ice thickness will increase, and a downstream stranding surface (with its population of direct falls) can be flushed further downstream, only to be stranded again and acquire a fresh brood of falls (*Cassidy et al.,* 1992; *Delisle and Sievers,* 1991).

3.7.4. Direct infall. Fresh meteorites fall directly onto recovery stranding surfaces, which can cause confusion if they are being added to a recently exposed paleo-stranding surface.

3.7.5. Recovery rate. One might assume that all meteorites from a given stranding surface can be easily recovered. However, considerable experience by the first author (M.E.Z.) indicates that meteorites are often missed due to the wind getting in a searcher's eyes, or burial by a transient snow patch. Meteorite recognition skills also vary considerably from person to person (even among veteran meteoriticists!), and luck plays a role. *Harvey* (1995) has discussed the problem of searching efficiency in some detail, and attempted to quantify a correction factor.

3.7.6. Weathering and differential survival of meteorites. Several factors have been identified that have major effects on the survival of meteorites on the ice. The chemical weathering of meteorites, although minimal in Antarctica by the cold and aridity, is still significant. Even while stored in ice, the action of thin monolayers of "unfrozen water" coating meteorites will inevitably cause chemical weathering (*Zolensky and Paces,* 1986). Meanwhile, ice movement can cause shearing and consequent breakage of the entrained meteorites (physical weathering). Finally, once the meteorites have emerged on the stranding surface, they are subject to accelerated chemical weathering on hot days when ice melts around them (the meteorites soak up solar radiation) and physical abrasion from the katabatic winds.

In "hot" deserts such as the Libyan Desert, Algeria, and Roosevelt County, New Mexico, the mean survival time of chondrites is >10 k.y. (*Boeckl,* 1972; *Jull et al.,* 1995; *Wlotzka et al.,* 1995a), although far older meteorites (~100 ka) are found in some fortuitous regions [e.g., Roosevelt County (see *Zolensky et al.,* 1992)].

Certain easily weathered meteorite types will be preferentially lost from the stranding record. Attempts to correct the Antarctic record for weathering effects (*Huss,* 1990a; *Harvey,* 1995) have had unknown success. *Bland et al.* (1996a,b) suggest that H chondrites weather faster than L chondrites (as might be expected from the former's greater metal content), although *Zolensky et al.* (1995) found just the opposite for meteorites recovered from the Atacama Desert. *Bland et al.* (1996a,b) point out that carbonates and hydrous silicates could, in some situations, armor mafic silicates and thereby provide a certain degree of protection against further alteration. Also, the changing temperature and aridity conditions attending regional climatic change would have further complicated this situation.

The main results of weathering will be threefold: (1) to decrease the population of all meteorites and reduce the mass of the survivors; (2) to increase the number of samples, through physical breakup, and subtly change the composition of the survivors (see below), increasing the importance and difficulty of pairing studies; and (3) removing from the record especially friable meteorites (e.g., CI1, of

which no Antarctic specimens have been found). Various workers have proposed correction factors for weathering, but these appear to be site specific (*Boeckl,* 1972; *Zolensky et al.,* 1992; *Harvey,* 1995).

3.7.7. Removal of meteorites by wind. The unrelenting katabatic winds in Antarctica promote rapid ablation [on the order of 5 cm/yr at the Allan Hills (*Schutt et al.,* 1986; *Cassidy et al.,* 1992)], and once meteorites emerge from the sublimating ice they are subject to transport downwind by these same winds (*Schutt et al.,* 1986; *Delisle and Sievers,* 1991; *Harvey,* 1995). This was elegantly demonstrated by an experiment at the Allan Hills main ice field. During the 1984–1985 field season, the NSF Antarctic Search for Meteorites (ANSMET) field party placed surrogate meteorites (rounded basalt samples of varying masses) onto a "starting line," one rock "team" sitting on the ice surface and the second team embedded just below the surface (*Schutt et al.,* 1986). This rock race was visited the following year, and the results were that all but the three largest buried meteorites had emerged. A number of stones were found to have moved downwind from the starting line, and eight had blown so far away that they could not be located.

Eolian effects are more pronounced in Antarctica than in other meteorite recovery regions, and the experiment described above has shown that specimen size inversely affects specimen movement, and that the mass threshold is a function of wind velocity, which relates to a specific area and may not be the same over different search regions. Small meteorites will be removed from the stranding surface by the action of wind alone, which undoubtedly skews the constitution of the recovered meteorite population.

3.7.8. Meteorite pairing. Many (most?) meteorites fall as showers of individuals that are subject to later breakage. In addition, physical weathering breaks meteorites into smaller, more numerous specimens. Flux calculations concern the number of individual falls, not total specimens, necessitating that meteorite pairing be determined. Pairing studies for unusual meteorites are well established; however, few of the ordinary chondrites (i.e., 90% of the collection) have received adequate study (because they are generally unexciting to most meteoriticists). Pairing for ordinary chondrites is most often done using comparative petrological, ^{26}Al, TL, and noble gas analyses (the latter revealing cosmic-ray-exposure histories) (*Schultz et al.,* 1991; *Benoit et al.,* 1993; *Scherer et al.,* 1995).

Unfortunately, as for the determination of terrestrial ages, no workers can analyze all meteorites on a given stranding surface, much less all 15,000 Antarctic specimens. In addition, weathering has been shown to deleteriously affect the noble gas content of chondrites, seriously complicating pairing studies (*Scherer et al.,* 1995). Therefore one must derive and apply a correction factor for the pairing of the ubiquitous ordinary chondrites; these have ranged from 2 to 6 (*Ikeda and Kimura,* 1992; *Lindstrom and Score,* 1995). Lindstrom and Score derived a chondrite pairing value of 5, based on the known pairing incidences of Antarctic meteorites. By applying this simple pairing correction value to the full population of Antarctic chondrites, they were able to address the question of possible differences in the meteorite population through time (see below).

Weathering the foregoing difficulties, workers have attempted to calculate the meteorite flux for Earth over the past several million years based upon the Antarctic meteorite record. As one example, *Huss* (1990a) concluded that that the ages of the Antarctic ice fields, as calculated from meteorite mass distributions, indicate an infall rate only slightly higher than the modern rate, concluding that the flux rate had not changed by more than a factor of 2 over the past million years. However, most agree that it is premature to attempt direct measurement of the past meteorite flux rate from the Antarctic record, despite the potential value in doing so. Additionally, considerable uncertainties exist in attempts to estimate the most critical variables, which continue to prevent accurate estimation of the flux. To advance this effort, the following studies should be undertaken: (1) The pairing of ordinary chondrites needs to be better constrained with real data. (2) We need to settle the nagging issue of the usefulness of TL in estimating meteorite terrestrial ages. (3) Investigation into the potential effects of weathering in the differential destruction of meteorite types, work begun now by Bland as described above, needs to continue. (4) Most critically, we need to better understand ice flow dynamics at each of the oldest meteorite stranding sites (Allan Hill and Lewis Cliff) to permit real meteorite fluxes to be calculated for the past 3 m.y.

Despite the difficulties faced in unraveling the record of past meteorite fluxes based on the record of the Antarctic meteorites, workers have also sought changes in the distribution of meteorite types among these same samples, as we shall see below.

3.8. More Ancient Meteorite Flux from Deposits of Fossil Meteorites

Quite surprisingly, more than 40 meteorites preserved in anoxic marls have lately been recovered from quarries in Scandinavia (*Schmitz et al.,* 1997, 2003). These "fossil" meteorites are recognizable due to pseudomorphed chondrule textures (Fig. 6) and preserved spinel grains with Al_2O_3/MgO and Al_2O_3/TiO_2 ratios similar to those in L and LL chondrites (Fig. 7). Workers have used the results of a systematic meteorite recovery operation from one particular quarry to attempt a calculation of chondrite flux some 420 m.y. ago (in the early Ordovician). As reported by *Schmitz et al.* (1997, 2003) this age is close to the calculated breakup age of the L-chondrite parent asteroid (420 ± 20 Ma). From a consideration of the number of recovered meteorites, the volume of material sampled, and sediment deposition rate, *Schmitz et al.* (1997, 2003) calculate an early Ordovician flux of L chondrites some 2 orders of magnitude greater than the modern rate. They further report, from these same sedimentary rocks, Os-isotopic and Ir contents consistent with an order of magnitude increase in the flux of interplanetary dust, ascribing this to the same L-

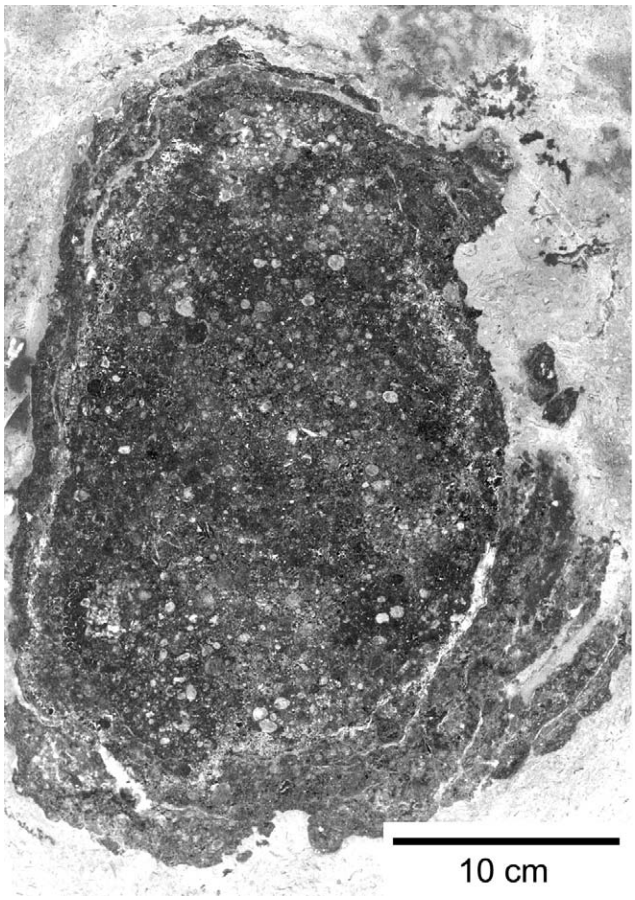

Fig. 6. Chondrule textures preserved in fossilized meteorites found in quarries in Scandinavia. After *Schmitz et al.* (2001). The millimeter- to submillimeter-sized round features apparent in this figure are fossil chondrules.

chondrite parent asteroid. Given their study assumptions, this report requires verification from another early Ordovician site (if this is even possible). However, if correct, this result suggests that directly upon breakup of the L-chondrite parent asteroid, Earth experienced a dramatic increase in L-chondrite falls. To generalize, the breakup of any body near Earth should temporarily increase the flux of extraterrestrial material — something that could and should have happened many times throughout Earth's history.

4. METEORITE TYPE STATISTICS

Where are meteorites coming from? How fast do these meteorite source regions evolve, as reflected in a changing complexion of meteorite types? What is the danger to life and structures from falling meteorites, and is this threat changing (*Beijing Observatory,* 1988)? Some geochronological techniques rely on a constant flux of extraterrestrial material to Earth — but how reasonable is this assumption? To discover the answers to these critical questions we need to determine the meteorite flux to Earth not just for the present day, but back into the past.

4.1. Meteorite Population Determinations from Falls

Without pressing a permanent force of persons into meteorite watch gangs, it is impossible to derive accurate meteorite fluxes from fall observations. But fall information probably does provide the best information on the relative types of meteorites that today pepper Earth (*Wasson,* 1985). Some workers suggest that the modern fall record favors

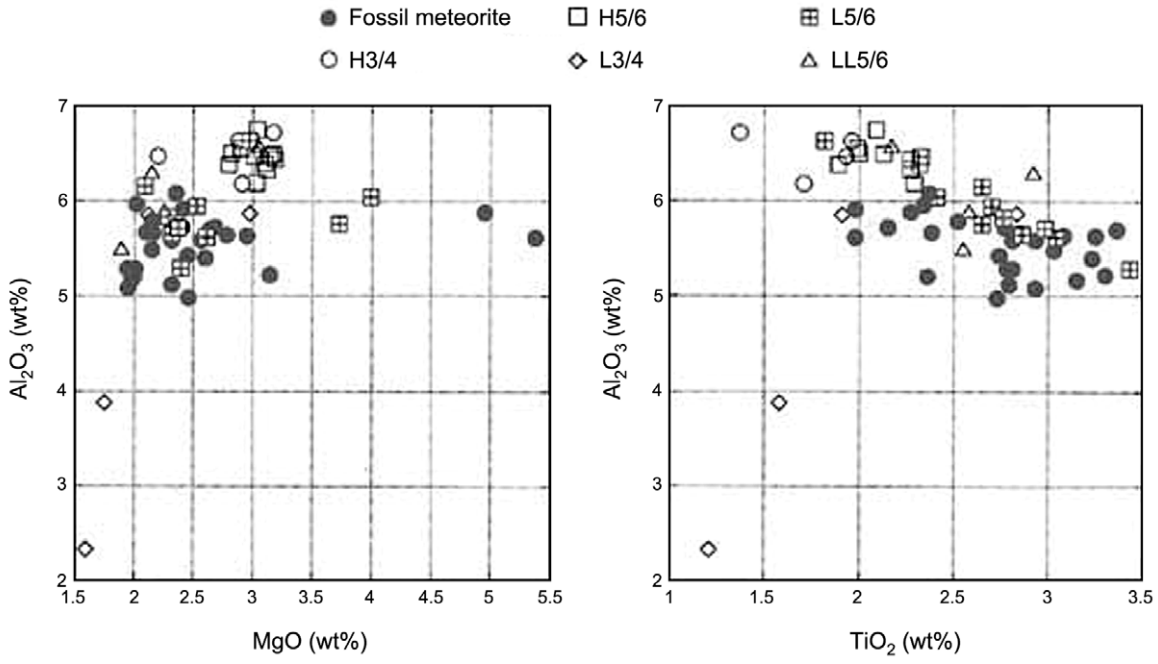

Fig. 7. Comparison of average chemical composition of chromite grains from 26 fossil meteorites and 33 ordinary chondrites. After *Schmitz et al*. (2001).

large showers over small, individual falls, but it is not clear what effect this potential bias would have. In any case, we wish to learn how fast the meteorite population changes, i.e., are we sampling different meteorite parent bodies through time?

4.2. Have Meteorite Populations Changed Through Time?

A very contentious subject has been that of potential compositional and mineralogical differences between younger finds and falls vs. older finds. An entire workshop was devoted to this subject (*Koeberl and Cassidy,* 1990). In particular, it appears that the important issue of possible observed changes in the H-chondrite populations remains unresolved.

In numerous papers, Wolf, Lipschutz, and coworkers argue that there is chemical evidence that Antarctic H4–6 and L4–6 chondrites with terrestrial ages >50 ka (from Victoria Land) are different from those that are younger (Queen Maud Land meteorites and modern falls) (*Dennison,* 1986; *Michlovich et al.,* 1995; *Wolf and Lipschutz,* 1995a,b,c). A difference between these meteorites would imply a change in the sources providing these meteorites over a timescale deemed too rapid by many dynamicists (*Wetherill,* 1986). Critics suggest that weathering may have redistributed the volatile trace elements being used for the difference arguments, but this view is disputed by some recent studies (*Wolf and Lipschutz,* 1995c; *Burns et al.,* 1995). Other critics point out that if it takes a sophisticated statistical examination of fully 10 trace elements in order to see a difference between the putative meteorite groups, then they are actually very similar. In a test of the Lipschutz-Wolf model, *Loeken and Schultz* (1995) performed analyses of noble gases in H chondrites from Antarctica (from Allan Hills and the Yamato Mountains) and modern falls. The authors were careful to select only Antarctic meteorites analyzed by Wolf and Lipschutz. They found no correlation between terrestrial age and either exposure age, radiogenic ^{4}He, or radiogenic ^{40}Ar over the period of the last 200 k.y. One might expect to see such correlations if the population source for Antarctic H-chondrite finds and modern H-chondrite falls indeed differed. Lipschutz and Wolf steadfastly maintained their position that the apparent population differences are real, and the reader will just have to decide the issue for himself.

As described above, *Lindstrom and Score* (1995) have examined the population statistics for the Antarctic meteorites recovered by the ANSMET expeditions. By applying a simple pairing correction value to the full population of Antarctic ordinary chondrites, they find that the relative numbers of Antarctic finds match modern fall statistics, so there is no difference in these populations when they are viewed in this manner (Table 1). Application of this simple pairing statistic suggests that there were approximately 1300 separate known Antarctic falls represented in the ANSMET collection in 1995. They also reported that most rare types of meteorites (with the exception of lunar and SNC meteorites) are small in mass.

TABLE 1. Meteorite populations for modern falls and Antarctic finds.

Meteorite Type	Modern Falls* (%)	Antarctic Finds† (%)
Ordinary chondrites	79.5	79.5
Carbonaceous chondrites	4.2	5.2
Enstatite chondrites	1.6	1.7
Achondrites	8.3	8.5
Stony irons	1.2	0.9
Irons	5.1	4.3
Total meteorites	830	1294

*From *Graham et al.* (1985)

†Numbers are given only for meteorites recovered by the ANSMET program. Data from *Lindstrom and Score* (1995), corrected for pairing (a pairing value of 5 was assumed for ordinary chondrites).

However, it is undeniable that a significant number of unique meteorites are found principally in Antarctica. These include lunar meteorites (all of which have been found in deserts, with the majority having been found in Antarctica), certain irons, CM1 chondrites, chondrite regolith breccias, and metamorphosed carbonaceous chondrites (*Zolensky et al.,* 2005). The majority of these unusual meteorites are small, under 1 kg, and it is undeniable that small meteorites are more likely to be recovered in Antarctica than elsewhere on Earth. This is despite the fact that small meteorites can be removed from stranding areas by the katabatic winds; those that remain are generally easily found, particularly in stranding areas devoid of terrestrial rocks. Nevertheless, it is intriguing that few of these types of meteorites have been found outside Antarctica.

As mentioned above, more than a dozen metamorphosed carbonaceous chondrites have been recognized from the Japanese Antarctic (JARE) collections, but only one has been recognized from the U.S. Antarctic collection (ANSMET), and there are none from modern falls or hot desert finds (*Zolensky et al.,* 2005). Typically the JARE meteorites have terrestrial ages intermediate between modern falls and meteorites recovered by ANSMET. This observation suggests that the source asteroid(s) of these metamorphosed carbonaceous chondrites may have broken up near Earth in the last 100,000 years. Recent modeling of such breakups show that they can signicifantly affect meteorite fluxes for up to 10^5 yr (*Gladman and Pauls*, 2005). These observations all require verification, but are sufficient to show that the flux rate and type of meteorites is not constant even at the scale of 10^5 yr.

4.3. Meteorite Masses

To a large degree the arguments for differences between Antarctic (old terrestrial age) and non-Antarctic (generally younger) meteorites comes down to the point that these unusual meteorites are generally small in size. It is certainly a fact that all Antarctic finds have smaller mean masses than comparable meteorites from the modern fall record (*Huss,* 1990a,b; *Harvey,* 1990, 1995; *Harvey and Cassidy,* 1991).

Four explanations for this latter observation are immediately apparent (others are undoubtedly also possible): (1) Small, unusual meteorites are falling today, but because they are small, are not generally recovered from most locales. Smaller meteorites are relatively easy to locate in Antarctica, due to the generally white to blue background and, locally, the low number of admixed terrestrial rocks. (2) Antarctic meteorites were identical to modern falls in mass, possibly different in type, and have been weathered into a steady-state population of smaller mass bits. (3) Antarctic meteorites are identical to modern falls, but the largest individuals have been preferentially removed from the Antarctic population, leaving only smaller specimens. Note that this would this make the Antarctic find record complementary to the modern fall record (where generally only the largest specimens are recovered). This explanation is, however, totally unsubstantiated by any reasonable mechanism. (4) The ancient meteorite flux was truly different from the modern one, in type and mass. Thus there are subtle indications that the old falls represented by the Antarctic collections have sampled a slightly different meteorite parent-body population. These differences are present at the 1–2% level of the total populations, however.

5. THE FLUX OF MICROMETEOROIDS TO EARTH

5.1. Satellite and Long Duration Exposure Facility Data

Satellite impact observations [such as the Long Duration Exposure Facility (LDEF) or Pegasus] only begin in the 1–100-mg range (*Humes,* 1991; *Naumann et al.,* 1966). For masses in the range of a few kilograms to tens of micrograms, available flux data are primarily camera, video, and radar observations of meteors. These techniques make use of the atmosphere as a detector. The major advantage of these approaches are the large collecting areas that can be utilized — up to 10^4 km^2 and higher for some radar and optical systems (cf. *Brown et al.,* 2002a,b; *Thomas et al.,* 1988). Each technique, however, suffers from different biases that make final flux interpretations somewhat problematic. For photographic/video observations, weather and daylight may bias accessible radiants and sensitivity is a function of angular velocity, making correction to a single limiting magnitude problematic (cf. *Hawkes,* 2002). Furthermore, these optical instruments detect radiation emitted by the meteor in the specific passband of the instrument — transforming to mass or size of the incident meteoroid requires knowledge of the luminous efficiency, a value that is poorly constrained over much of the size/velocity range of interest (cf. *Bronsthen,* 1983, for a review). These physical uncertainties are further compounded by the general logistical difficulty of running optical networks for long periods (and reducing the resulting data); the few successful examples are the three large fireball networks (*Halliday et al.,* 1989), of which only the European Network is still in operation (*Spurný,* 1997). Video systems (which access a smaller particle population than the camera networks) operating continuously are just now becoming feasible with faster computers and cheap, mass-storage devices being developed.

Radar systems suffer a greater range of biases than optical instruments, including poorly known ionization efficiencies, fragmentation effects, recombination, and initial radius biases (*Baggaley,* 2002). In addition, most backscatter meteor radar observations reflect off a small segment (1–2 km) of the meteor trail only and so can provide (at best) a limiting value for the mass of any particular incident meteoroid. Historically, underestimation of the effects of the initial trail radius bias have led to radar influx measurements more than an order of magnitude smaller than comparable satellite measurements at the same mass (*Hughes,* 1980, 1994). Low-frequency radar observations (*Thomas et al.,* 1988) and modeling of this effect (*Campbell-Brown and Jones,* 2003) have led to flux estimates more consistent with dust detector values. Computation of the radar collecting area is also more complicated than is the case for optical instruments (*Brown and Jones,* 1995). Technically, radars also tend to be labor intensive to operate and maintain; however, once working and with suitable processing algorithms they are best suited for long-term surveys and tend to produce much larger datasets, in some cases exceeding 10^4 meteor echoes per day (*Baggaley,* 2002). Cross-calibration of optical and radar measurements of meteors is a major outstanding issue to address the flux at masses of micrograms to milligrams.

Examination of Fig. 8 shows the flux measurements available in the 10–10^{-5} g range (meteoroids to micrometeoroids). Most remarkable is the lack of modern measurements over much of this range; no dedicated optical sporadic meteor fluxes have been made using video or CCD instruments, and only LDEF satellite data covers the lower decade in mass. *Hawkins* (1960) used Super-Schmidt camera data to compute meteor fluxes at bright (+2 and brighter) visual magnitudes, although these are based on a relatively small sample and suffer from the uncertainties in panchromatic luminous efficiencies at these sizes (cf. *Ceplecha et al.,* 1998). Among the best modern meteor radar measurements are those from the high-power, low-frequency Jindalee radar (*Thomas and Netherway,* 1989). These data are particularly suited to flux determinations as the low frequencies involved produce negligible initial radius biases, are less affected by fragmentation interference effects, and the collecting area for the system is well-determined. The estimated flux from this source is also shown in Fig. 8.

Ceplecha (2001) has produced a compendium of primary data sources over this mass interval, although the exact reduction technique used to transform to final flux values is not discussed in detail (see Fig. 8). Ceplecha's flux curve is generally below that found from *Hawkins* (1960) values and also below the standard *Grün et al.* (1985) interplanetary dust flux model, which is itself based on earlier Apollo-era satellite and radar meteor data.

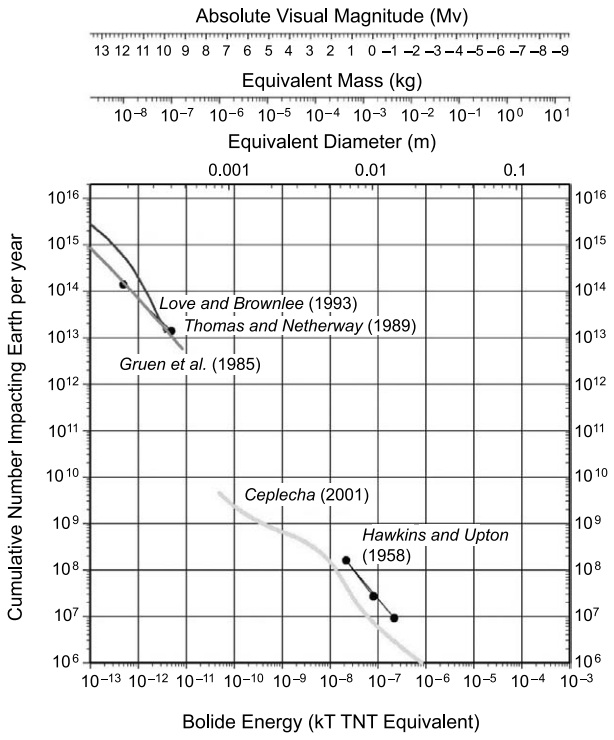

Fig. 8. Flux measurements available in the 10^{-8}–10-kg range. The same velocity and bulk density assumptions are used as in Fig. 9. The equivalent absolute visual magnitude is found following the relation given by *Verniani* (1973). Among the best modern meteor radar measurements are those from the high-power, low-frequency Jindalee radar [*Thomas and Netherway* (1989), triangles in the upper left portion of the figure], which suffers much less from biases that heavily affect higher-frequency meteor radar meteor flux measurements. The standard interplanetary flux curve produced by *Grün et al.* (1985) from a compilation of satellite impact data and other sources is also shown as a thick black line. The flux derived from impact craters measured on LDEF (*Love and Brownlee,* 1993) is given up to the size of the largest equivalent impactor near 10^{-7} kg. The compilation of *Ceplecha* (2001) based on video and photographic observations (thick gray line) is also shown (valid for masses >10^{-6} kg). Measurements of Super-Schmidt meteors by *Hawkins and Upton* (1958) (solid circles) differ from that of *Ceplecha* (2001), in part due to differences in the mass scaling used to convert luminous intensity to mass. This uncertainty in the optical mass scale may also partially explain the apparent gap between the *Ceplecha* (2001) curve and the measurements valid for m < 10^{-7} kg. The *Halliday et al*. (1996) fireball curve shown in Fig. 9 is also given for comparison. *Hawkins* (1960) used Super-Schmidt camera data to compute meteor fluxes at bright (+2 and brighter) visual magnitudes, although these are based on a relatively small sample and suffer from the uncertainties in panchromatic luminous efficiencies at these sizes (cf. *Ceplecha et al.,* 1998).

Numerous datasets from satellite impact detectors and/or returned surfaces have provided micrometeoroid flux estimates in the <10^{-4}-g mass range (cf. *Staubach et al.,* 2001, for a review). Results from LDEF, in particular, provide the largest time-area exposure product of any dataset to date. The micrometeoroid flux from LDEF returned surfaces have been determined by counting the cumulative number vs. size for visible impact craters on the space-facing end of the returned satellite surface (*Love and Brownlee,* 1993). Laboratory calibration of impact crater depth-diameter-impactor density-velocity relations permit reconstruction of the original particle mass. The original LDEF micrometeoroid flux curve measured by *Love and Brownlee* (1993) is shown in Fig. 8.

One crucial assumed input parameter in this analysis (and others that use satellite measurements to infer impactor masses) is meteoroid velocity. To date, accurate individual meteoroid velocities have only been measured for meteoroids impacting Earth's atmosphere. Historically, mass-averaged velocities derived from the Harvard Radio Meteor Project (*Sekanina and Southworth,* 1975) or the photographically inferred velocity distribution for larger meteoroids (*Erickson,* 1968) have been used. The *Erickson* (1968) distribution is appropriate to large meteoroids (gram-sized and larger) and is based on less than 300 meteors total. There are less than 65 meteors with velocities in excess of 50 km/s in this survey. The original HRMP velocity distribution has also been found to be in error by 2 orders of magnitude at higher velocities due to a typographic error (*Taylor and Elford,* 1998). The revised HRMP velocity distribution pushes the mass-averaged normal velocities from 12 km/s as used in the LDEF analysis to 18 km/s. This has the effect of shifting the LDEF flux curve downward by a factor of 2 in mass.

More recently, two independent radar surveys, one in the southern hemisphere (*Galligan and Baggaley,* 2004) and one in the northern hemisphere (*Brown et al.,* 2005), have remeasured velocities for faint radar meteors using a technique different from that utilized by the HRMP (see Fig. 9). Both find that the mass-averaged mean velocity is much higher than the original HRMP value of 14 km/s (*Southworth and Sekanina,* 1973). This may represent an unrecognized bias against fragmenting meteors in the original HRMP survey due to the velocity measurement technique. If this finding is confirmed, the effect will be to move the mass flux curve for microgram and smaller measurements downward by close to an order of magnitude at some masses. Remaining differences between the various velocity distributions as shown in Fig. 9 may reflect differences in the choice of bias-correction terms.

There have been several attempts to determine the composition of meteoroids and micrometeoroids of cometary origin by averaging the composition of the radiating gas along the fireball path (e.g., *Ceplecha,* 1964, 1965; *Millman,* 1972; *Harvey,* 1973; *Nagasawa,* 1978; *Borovička,* 1993; *Borovička and Spurný,* 1996; *Borovička and Betlem,* 1997; *Ceplecha et al.,* 1998). The most recent study (*Trigo-Rodriguez et al.,* 2004a,b) suggests that these meteoroids have Si-normalized compositions of most determined elements (Mg, Fe, Ni, Cr, Mn, and Co) in the range of the CM and CI chondrites, but exhibited depletions in Ca and Ti,

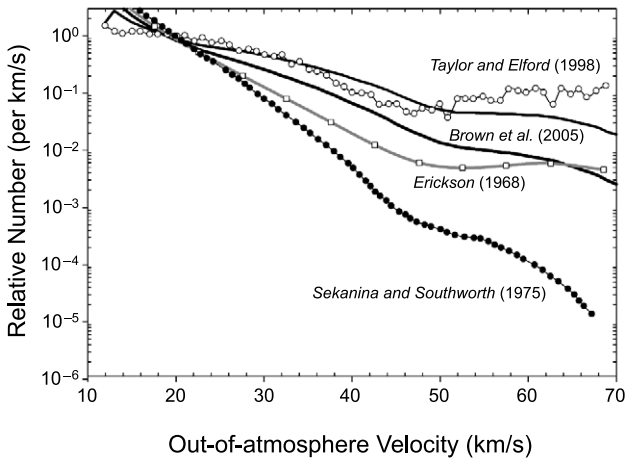

Fig. 9. The velocity distribution of meteoroids at Earth as measured by two radar surveys and from photographic observations. All data are normalized to the number of meteoroids measured in the 20 km/s velocity bin. The solid circles are the measured velocity distribution from the Harvard Radio Meteor Project (HRMP) as published by *Sekanina and Southworth* (1975), which has been used extensively in the literature (e.g., *Love and Brownlee,* 1993). The open circles are the revision of these same data using modern correction factors by *Taylor and Elford* (1998). The solid lines represent the upper and lower error limits of the distribution measured by the Canadian Meteor Orbit Radar (*Brown et al.,* 2005). Photographic estimates of the velocity distribution from Super-Schmidt camera measurements by *Erickson* (1968) are shown for comparison. Both sets of radar data are applicable to meteoroid masses in the 10^{-4}–10^{-5}-g range, while the photographic data represent meteoroids with masses on the order of 1 g.

ascribed to incomplete volatilization of these elements. Surprisingly, the meteoroids appeared to have a factor of 2–3 greater Na than CI or CM chondrites and even chondritic IDPs of probably cometary origin. They suggest that this Na enrichment is real, and that Na has been removed from the IDPs by atmospheric heating. Hopefully, the cometary dust being returned to Earth in January 2006 by the Stardust mission will help settle this issue.

5.2. Past Dust Flux

Since most of the ^{3}He in ocean sediments derives from IDPs, its concentration can be used as a sensor of the flux of IDPs back through time. As for the meteorite record in Earth's geologic column, there is also evidence that the flux of extraterrestrial dust to Earth has not been constant in even the recent geologic past. The ^{3}He concentrations in slowly accumulating pelagic clays suggest considerable changes (up to 5×) in the IDP flux over the past 70 m.y. (*Farley,* 1995) (Fig. 10). The pronounced peak in ^{3}He at approximately 8 Ma appears to correspond to the breakup of the Veritas family progenitor asteroid, which is the most recent of the major asteroid breakup events. It has been estimated that as much as 25% of the IDPs reaching Earth today derive from this family (W. Bottke, personal communication, 2005), but it is clear from the ^{3}He spike that immediately following the impact event that created and dispersed the Veritas family asteroids, dust from this source dominated the flux to Earth. Since the asteroids in this family are type Ch (i.e., C-type asteroids containing appreciable hydrated minerals), this dust would have brought a significant quantity of water to Earth over the past 8 m.y.

In addition, there appears to be an approximately 100-k.y. periodicity in ^{3}He concentration back though at least the past 500 k.y. (*Muller and MacDonald,* 1995; *Farley and Patterson,* 1995) (Fig. 11). The cause of the apparent periodicity remains unexplained.

6. SUMMARY

All measurements of the present fluxes of extraterrestrial materials can be combined with the measured and calculated fluxes of entire asteroids and comets to Earth (crater-forming objects) into a single diagram (Fig. 12). As we

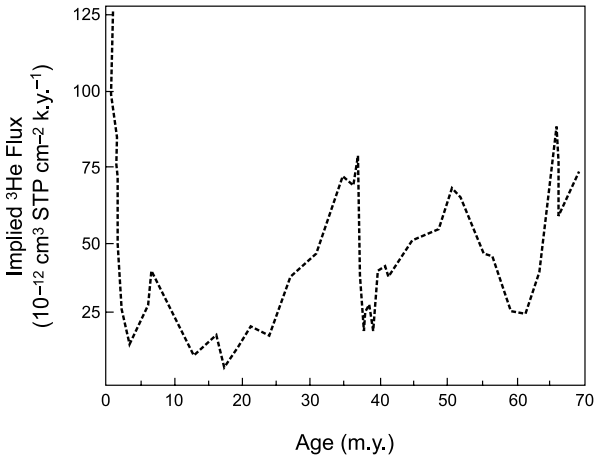

Fig. 10. The ^{3}He concentrations in slowly accumulating pelagic clays suggest considerable changes (up to 5×) in the IDP flux over the past 70 m.y. (after *Farley,* 1995).

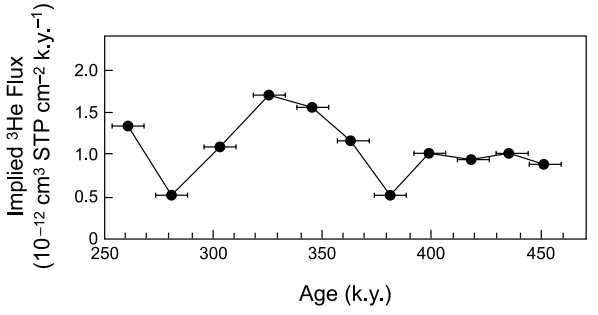

Fig. 11. There appears to be an approximately 100-k.y. periodicity in ^{3}He concentration over at least the past 500 k.y. (after *Farley and Patterson,* 1995).

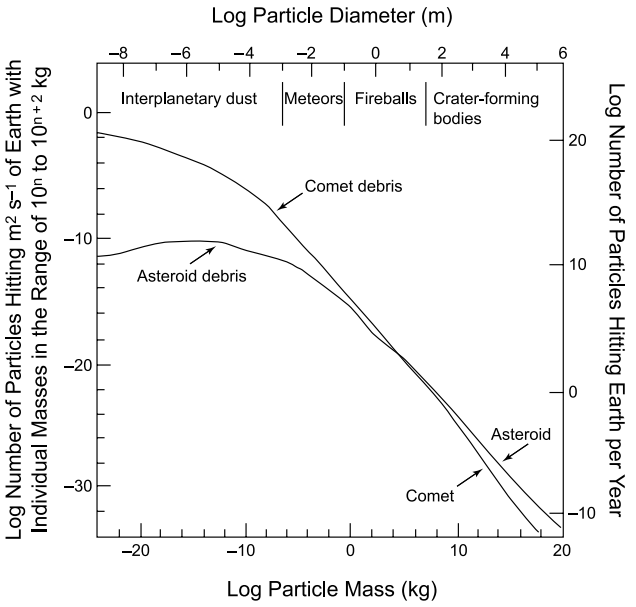

Fig. 12. Histogram showing the annual flux of extraterrestrial material to Earth (after *Hughes,* 1994). The flux is divided into four regions: IDPs and micrometeorites, meteors, fireballs, and crater-forming bodies.

have seen, the flux of meteorite and smaller-sized objects has varied considerably over the recent geologic past, and so the diagram in Fig. 12 is accurate only for the present. Future studies will shed additional light on the types and magnitudes of changes to this flux in the past.

REFERENCES

Annexstad J., Schultz L., and Zolensky M. E., eds. (1995) *Workshop on Meteorites From Cold and Hot Deserts.* LPI Tech. Rpt. 95-02, Lunar and Planetary Institute, Houston. 83 pp.

Aylmer D., Bonanno V., Herzog G. F., Weber H., Klein J., and Middleton R. (1988) Al-26 and Be-10 production in iron meteorites. *Earth Planet. Sci. Lett., 88,* 107–118.

Baggaley W. J. (2002) Radar observations. In *Meteors in the Earth's Atmosphere* (E. Murad and I. P. Williams, eds.), p. 123. Cambridge Univ., Cambridge.

Beijing Observatory, ed. (1988) *Zhongguo Gudai Tianxiang Jilu Zongji* (*A Union Table of Ancient Chinese Records of Celestial Phenomena*), pp. 63–105. Kexue Jishu Chubanshe, Kiangxu.

Benoit P. H., Sears H., and Sears D. W. G. (1992) The natural thermoluminescence of meteorites. 4. Ordinary chondrites at the Lewis Cliff Ice Field. *J. Geophys. Res., 97,* 4629–4647.

Benoit P. H., Sears H., and Sears D. W. G. (1993) The natural thermoluminescence of meteorites. 5. Ordinary chondrites at the Allan Hills Ice Fields. *J. Geophys. Res., 98,* 1875–1888.

Benoit P. H., Roth J., Sears H., and Sears D. W. G. (1994) The natural thermoluminescence of meteorites. 7. Ordinary chondrites from the Elephant Moraine region, Antarctica. *J. Geophys. Res., 99,* 2073–2085.

Binzel R. P., Lupishko D., di Martino M., Whiteley R. J., and Hahn G. J. (2002) Physical properties of near-Earth objects. In *Asteroids III* (W. F. Bottke Jr. et al., eds.), pp. 255–271. Univ. of Arizona, Tucson.

Binzel R P., Rivkin A. S., Stuart J. S., Harris A. W., Bus S. J., and Burbine T. H. (2004) Observed spectral properties of near-Earth objects: Results for population distribution, source regions, and space weathering processes. *Icarus, 170,* 259–294.

Bland P. A. and Artemieva N. A. (2003) Efficient disruption of small asteroids by Earth's atmosphere. *Nature, 424,* 288–291.

Bland P., Berry F. J., Smith T. B., Skinner S. J., and Pillinger C. T. (1996a) The flux of meteorites to the Earth and weathering in hot desert ordinary chondrite finds. *Geochim. Cosmochim. Acta, 60,* 2053–2059.

Bland P., Smith T. B., Jull A. J. T., Berry F. J., Bevan A. W. R, Cloud S., and Pillinger C. T. (1996b) The flux of meteorites to the Earth over the last 50,000 years. *Mon. Not. R. Astron. Soc., 283,* 551–565.

Bland P. A., Zolensky M. E., Benedix G. K., and Sephton M. A. (2006) Weathering of chondritic meteorites. In *Meteorites and the Early Solar System II* (D. S. Lauretta and H. Y. McSween Jr., eds.), this volume. Univ. of Arizona, Tucson.

Boeckl R. (1972) Terrestrial age of nineteen stony meteorites derived from their radiocarbon content. *Nature, 236,* 25–26.

Borovička J. (1993) A fireball spectrum analysis. *Astron Astrophys., 279,* 627–645.

Borovička J. and Betlem H. (1997) Spectral analysis of two Perseid meteors. *Planet. Space Sci., 45,* 563–575.

Borovička J. and Kalenda P. (2003) The Moravka meteorite fall: 4. Meteoroid dynamics and fragmentation in the atmosphere. *Meteoritics & Planet. Sci., 38,* 1023–1043.

Borovička J. and Spurný P. (1996) Radiation study of two very bright terrestrial bolides. *Icarus, 121,* 484–510.

Borovička J., Weber H. W., Jopek T., Jakes P., Randa Z., Brown P. G., ReVelle D. O., Kalenda P., Schultz L., Kucera J., Haloda J., Tycova P., Fryda J., and Brandstatter F. (2003) The Moravka meteorite fall: 3. Meteoroid initial size, history, structure, and composition. *Meteoritics & Planet. Sci., 38,* 1005–1021.

Bronshten V. A. (1983) *Physics of Meteor Phenomena.* Reidel, Dordrecht. 356 pp.

Brown H. (1960) The density and mass distribution of meteoritic bodies in the neighbourhood of the Earth's orbit. *J. Geophys. Res., 65,* 1679–1683.

Brown H. (1961) Addendum: The density and mass distribution of meteoritic bodies in the neighbourhood of the Earth's orbit. *J. Geophys. Res., 66,* 1316–1317.

Brown P. and Jones J. (1995) A determination of the strengths of the sporadic radio-meteor sources. *Earth Moon Planets, 68,* 223–245.

Brown P., Hildebrand A. R., Green D. W. E., Page D., Jacobs C., ReVelle D., Tagliaferri E., Wacker J., and Wetmiller B. (1996) The fall of the St-Robert meteorite. *Meteoritics & Planet. Sci., 31,* 502–517.

Brown P., Spalding R. E., ReVelle D. O., Tagliaferri E., and Worden S. P. (2002a) The flux of small near-Earth objects colliding with the Earth. *Nature, 420,* 294–296.

Brown P., Campbell M. D., Hawkes R. L., Theijsmeijer C., and Jones J. (2002b) Multi-station electro-optical observations of the 1999 Leonid meteor storm. *Planet. Space Sci., 50,* 45–55.

Brown P., Jones J., Weryk W. J., and Campbell-Brown M. D. (2005) The velocity distribution of meteoroids at the earth as measured by the Canadian meteor orbit radar (CMOR). *Earth Moon Planets,* in press.

Buchwald V. F. (1975) *Handbook of Iron Meteorites, Volume 1: Iron Meteorites in General*. Univ. of California, Berkeley.

Burns R. G., Burbine T. H., Fisher D. S., and Binzel R. P. (1995) Weathering in Antarctic H and CR chondrites: Quantitative analysis through Mössbauer spectroscopy. *Meteoritics, 30,* 625–633.

Campbell-Brown M and Jones J. (2003) Determining the initial radius of meteor trains. *Mon. Not. R. Astron. Soc., 343,* 3.

Cassidy W., Harvey R., Schutt J., Delisle G., and Yanai K. (1992) The meteorite collection sites of Antarctica. *Meteoritics, 27,* 490–525.

Ceplecha Z. (1964) Study of a bright meteor flare by mean of emission curve of growth. *Bull. Astron. Inst. Czech., 15,* 102–112.

Ceplecha Z. (1965) Complete data on bright meteor 32281. *Bull. Astron. Inst. Czech., 16,* 88–101.

Ceplecha Z. (1994) Impacts of meteoroids larger than 1 m into the Earth's atmosphere. *Astron. Astrophys., 286,* 967–970.

Ceplecha Z. (2001) The meteoroidal influx to the Earth. In *Collisional Processes in the Solar System* (M. Ya. Marov and H. Rickman, eds.), pp. 35–50. Astrophysics and Space Science Series Vol. 261, Kluwer, Dordrecht.

Ceplecha Z., Borovička J., Elford W. G., ReVelle D. O., Hawkes R. L., Porubcan V., and Simek M. (1998) Meteor phenomena and bodies. *Space Sci. Rev., 84,* 327–471.

Chang C. T. and Wänke H. (1969) Beryllium-10 in iron meteorites, their cosmic ray exposure and terrestrial ages. In *Meteorite Research* (P. M. Millman, ed.), pp. 397–406. Reidel, Dordrecht.

Delisle G. (1993) Global change, Antarctic meteorite traps and the East Antarctic ice sheet. *J. Glaciol., 39,* 397–408.

Delisle G. (1995) Storage of meteorites in Antarctic ice during glacial and interglacial stages. In *Workshop on Meteorites from Cold and Hot Deserts* (L. Schultz et al., eds.), pp. 26–27. LPI Tech. Rpt. 95-02, Lunar and Planetary Institute, Houston.

Delisle G. and Sievers J. (1991) Sub-ice topography and meteorite finds near the Allan Hills and the Near Western Ice Field, Victoria Land, Antarctica. *J. Geophys. Res., 96,* 15577–15587.

Dennison J. E., Ligner D. W., and Lipschutz M. E. (1986) Antarctic and non-Antarctic meteorites form different populations. *Nature, 319,* 390–393.

Drummond J. D. (1991) Earth-approaching asteroid streams. *Icarus, 89,* 14–25.

Erickson J. E. (1968) Velocity distribution of sporadic photographic meteors. *J. Geophys. Res., 73,* 3721–3762

Farley K. A. (1995) Cenozoic variations in the flux of interplanetary dust recorded by ^{3}He in a deep-sea sediment. *Nature, 376,* 153–156.

Farley K. A. and Patterson D. B. (1995) A 100-kyr periodicity in the flux of extraterrestrial ^{3}He to the sea floor. *Nature, 378,* 600–603.

Fireman E. L. (1983) Carbon-14 ages of Allan Hills meteorites and ice (abstract). In *Lunar and Planetary Science XIV,* pp. 195–196. Lunar and Planetary Institute, Houston.

Freundel M., Schultz L., and Reedy R. C. (1986) Terrestrial ^{81}Kr-Kr ages of Antarctic meteorites. *Geochim. Cosmochim. Acta, 50,* 2663–2673.

Galligan D. P. and Baggaley W. J. (2004) The orbital distribution of radar-detected meteoroids of the solar system dust cloud. *Mon. Not. R. Astron. Soc., 353,* 422–446.

Gladman B. and Pauls A. (2005) Decoherence scales for meteoroid streams (abstract). In *Asteroids, Comets and Meteors,* p. 66. IAU Symposium No. 229.

Graham A. L., Bevan A. W. R., and Hutchison R. (1985) *Catalogue of Meteorites*. Univ. of Arizona, Tucson.

Grün E., Zook H., Fechtig H., and Giese R. H. (1985) Collisional balance of the meteoritic complex. *Icarus, 62,* 244–272.

Halliday I. (1987) Detection of a meteorite stream: Observations of a second meteorite fall from the orbit of the Innisfree chondrite. *Icarus, 69,* 550–556.

Halliday I., Blackwell A. T., and Griffin A. A. (1978) The Innisfree meteorite and the Canadian camera network. *J. R. Astron. Soc. Canada, 72,* 15–39.

Halliday I., Griffin A. A., and Blackwell A. T. (1981) The Innisfree meteorite fall: A photographic analysis of fragmentation, dynamics and luminosity. *Meteoritics, 16,* 153–170.

Halliday I., Blackwell A. T., and Griffin A. A. (1984) The frequency of meteorite falls on the Earth. *Science, 223,* 1405–1407.

Halliday I., Blackwell A. T., and Griffin A. A. (1989) The flux of meteorites on the Earth's surface. *Meteoritics, 24,* 173–178.

Halliday I., Blackwell A. T., and Griffin A. A. (1991) The frequency of meteorite falls: Comments on two conflicting solutions to the problem. *Meteoritics, 26,* 243–249.

Halliday I., Griffin A. A., and Blackwell A. T. (1996) Detailed data for 259 fireballs from the Canadian camera network and inferences concerning the influx of large meteoroids. *Meteoritics, 31,* 185–217.

Harvey G. A. (1973) Elemental abundance determinations for meteors by spectroscopy. *J. Geophys. Res., 78,* 3913–3926.

Harvey R. P. (1990) Statistical differences between Antarctic finds and modern falls: Mass frequency distributions and relative abundance by type. In *Workshop on Differences Between Antarctic and Non-Antarctic Meteorites* (C. Koeberl and W. A. Cassidy, eds.), pp. 43–45. LPI Tech. Rept. 90-01, Lunar and Planetary Institute, Houston.

Harvey R. P. (1995) Moving targets: The effect of supply, wind movement, and search losses on Antarctic meteorite size distributions. In *Workshop on Meteorites from Cold and Hot Deserts* (L. Schultz et al., eds.), pp. 34–37. LPI Tech. Rpt. 95-02, Lunar and Planetary Institute, Houston.

Harvey R. P. and Cassidy W. A. (1991) A statistical comparison of Antarctic finds and modern falls: Mass frequency distributions and relative abundance by type. *Meteoritics, 24,* 9–14.

Harris A. W. (2002) A new estimate of the population of small NEAs. *Bull. Am. Astron. Soc., 34,* 835.

Hawkes R. L. (2002) Detection and analysis procedures for visual, photographic and image intensified CCD meteor observations. In *Meteors in the Earth's Atmosphere* (E. Murad and I. Williams, eds.), p. 97. Cambridge Univ., Cambridge.

Hawkins G. S. (1960) Asteroidal fragments. *Astron. J., 65,* 318–322.

Hawkins G. S. and Upton E. K. L. (1958) The influx rate of meteors in the Earth's atmosphere. *Astrophys. J., 128,* 727–735.

Honda M. and Arnold J. R. (1964) Effects of cosmic rays on meteorites. *Science, 143,* 203–212.

Hughes D. W. (1980) On the mass distribution of meteorites and their influx rate. In *Solid Particles in the Solar System* (I. Halliday and B. A. McIntosh, eds.), pp. 207–210. Reidel, Dordrecht.

Hughes D. W. (1994) Comets and asteroids. *Contemporary Phys., 35,* 75–93.

Humes D. (1991) Large craters on the Meteoroid and Space De-

bris Impact Experiment. In *LDEF, 69 Months in Space: First Post-Retrieval Symposium* (A S. Levine, ed.), p. 399. NASA, Washington, DC.

Huss G. (1990a) Meteorite infall as a function of mass: Implications for the accumulation of meteorites on Antarctic ice. *Meteoritics, 25,* 41–56.

Huss G. (1990b) Meteorite mass distributions and differences between Antarctic and non-Antarctic meteorites. In *Workshop on Differences Between Antarctic and Non-Antarctic Meteorites* (C. Koeberl and W. A. Cassidy, eds.), pp. 49–53. LPI Tech. Rpt. 90-01, Lunar and Planetary Institute, Houston.

Huss G. (1991) Meteorite mass distribution and differences between Antarctic and non-Antarctic meteorites. *Geochim. Cosmochim. Acta, 55,* 105–111.

Ikeda Y. and Kimura M. (1992) Mass distribution of Antarctic ordinary chondrites and the estimation of the fall-to-specimen ratios. *Meteoritics, 27,* 435–441.

Jenniskens P., Wilson M. A., Packan D., Laux C. O., Krüger C. H., Boyd I. D., Popova O. P., and Fonda M. (2000) Meteors: A delivery mechanism of organic matter to the early Earth. *Earth Moon Planets, 82/83,* 57–70.

Jopek T. J., Valsecchi G. B., and Froeschlé C. (2002) Asteroid meteoroid streams. In *Asteroids III* (W. F. Bottke Jr. et al., eds.), pp. 645–652. Univ. of Arizona, Tucson.

Jull A. J. T., Wlotzka F., Palme H. and Donahue D. J. (1990) Distribution of terrestrial age and petrologic type of meteorites from western Libya. *Geochim. Cosmochim. Acta, 54,* 2895–2898.

Jull A. J. T., Donahue D. J., Cielaszyk E., and Wlotzka F. (1993a) Carbon-14 terrestrial ages and weathering of 27 meteorites from the southern high plains and adjacent areas (USA). *Meteoritics, 28,* 188–195.

Jull A. J. T., Wloztka F., Bevan A. W. R., Brown S. T., and Donahue D. J. (1993b) ^{14}C terrestrial ages of meteorites from desert regions: Algeria and Australia. *Meteoritics, 28,* 376–377.

Jull T., Bevan A. W. R., Cielaszyk E., and Donahue D. J. (1995) Carbon-14 terrestrial ages and weathering of meteorites from the Nullarbor region, Western Australia. In *Workshop on Meteorites from Cold and Hot Deserts* (L. Schultz et al., eds.), pp. 37–38. LPI Tech. Rpt. 95-02, Lunar and Planetary Institute, Houston.

Koeberl C. and Cassidy W. A., eds. (1990) *Workshop on Differences Between Antarctic and Non-Antarctic Meteorites*. LPI Tech. Rpt. 90-01, Lunar and Planetary Institute, Houston. 102 pp.

Lindstrom M. and Score R. (1995) Populations, pairing and rare meteorites in the U.S. Antarctic meteorite collection. In *Workshop on Meteorites from Cold and Hot Deserts* (L. Schultz et al., eds.), pp. 43–45. LPI Tech. Rpt. 95-02, Lunar and Planetary Institute, Houston.

Loeken M. and Schultz L. (1995) The noble gas record of H chondrites and terrestrial age: No correlation. In *Workshop on Meteorites from Cold and Hot Deserts* (L. Schultz et al., eds.), pp. 45–47. LPI Tech. Rpt. 95-02, Lunar and Planetary Institute, Houston.

Love S. G. and Brownlee D. E. (1993) A direct measurement of the terrestrial mass accretion rate of cosmic dust. *Science, 262,* 550–553.

McCrosky R. E. and Ceplecha Z. (1969) Photographic networks for fireballs. In *Meteorite Research* (P. M. Millman, ed.), pp. 600–612. Reidel, Dordrecht.

Michlovich E. S., Wolf S. F., Wang M.-S., Vogt S., Elmore D., and Lipschutz M. (1995) Chemical studies of H chondrites. 5. Temporal variations of sources. *J. Geophys. Res., 100,* 3317–3333.

Millard H. T. Jr. (1963) The rate of arrival of meteorites at the surface of the Earth. *J. Geophys. Res., 68,* 4297–4303.

Millman P. M. (1972) Giacobinid meteor spectra. *J. R. Astron. Soc. Canada, 66,* 201–211.

Muller R. A. and MacDonald G. (1995) Glacial cycles and orbital inclination. *Nature, 377,* 107–108.

Nagasawa K. (1978) Analysis of spectra of Leonid meteors. *Ann. Tokyo Astron. Obs. 2nd Series, 16,* 157–187.

Naumann N. R. J. (1966) *The Near Earth Meteoroid Environment.* NASA TND 3717, U.S. Government Printing Office, Washington, DC.

Nemtchinov I. V., Svetsov V. V., Kosarev I. B., Golub A. P., Popova O. P., Shuvalov V. V., Spalding R. E., Jacobs C., and Tagliaferri E. (1997) Assessment of kinetic energy of meteoroids detected by satellite-based light sensors. *Icarus, 130,* 259–274.

Nishiizumi K. (1990) Update on terrestrial ages of Antarctic meteorites. In *Antarctic Meteorite Stranding Surfaces* (W. A. Cassidy and I. M. Whillans, eds.), pp. 49–53. LPI Tech. Rpt. 90-03, Lunar and Planetary Institute, Houston.

Nishiizumi K. (1995) Terrestrial ages of meteorites from cold and cold regions. In *Workshop on Meteorites from Cold and Hot Deserts* (L. Schultz et al., eds.), pp. 53–55. LPI Tech. Rpt. 95-02, Lunar and Planetary Institute, Houston.

Nishiizumi K., Elmore D., and Kubik P. W. (1989a) Update on terrestrial ages of Antarctic meteorites. *Earth Planet. Sci. Lett., 93,* 299–313.

Nishiizumi K., Winter E., Kohl C., Klein J., Middleton R., Lal D., and Arnold J. (1989b) Cosmic-ray production rates of Be-10 and Al-26 in quartz from glacially polished rocks. *J. Geophys. Res.–Solid Earth and Planets, 94,* 17907–17915.

Rabinowitz D. L. et al. (1993) Evidence for a near-Earth asteroid belt. *Nature, 363,* 704–706.

Rabinowitz D., Helin E., Lawrence K., and Pravdo S. (2000) A reduced estimate of the number of kilometer-sized near-Earth asteroids. *Nature, 403,* 165–166.

Rawcliffe R. D., Bartky C. D., Gordon E., and Carta D. (1974) Meteor of August 10, 1972. *Nature, 247,* 284–302.

ReVelle D. O. (1997) Historical detection of atmospheric impacts of large super-bolides using acoustic-gravity waves. *Ann. N. Y. Acad. Sci., 822,* 284–302

Scherer P., Schultz L., Neupert U., Knauer M., Neumann S., Leya I., Michel R., Mokos J., Lipschutz M. E., Metzler K., Suter M., and Kubik P. W. (1987) Allan Hills 88019: An Antarctic H-chondrite with a very long terrestrial age. *Meteoritics & Planet. Sci., 32,* 769–773.

Scherer P., Schultz L., and Loeken Th. (1995) Weathering and atmospheric noble gases in chondrites from hot deserts. In *Workshop on Meteorites from Cold and Hot Deserts* (L. Schultz et al., eds.), pp. 58–60. LPI Tech. Rpt. 95-02, Lunar and Planetary Institute, Houston.

Schmitz B., Peucker-Ehrenbrink B., Lindström M., and Tassinari M. (1997) Accretion rates of meteorites and cosmic dust in the early Ordovician. *Science, 278,* 88–90.

Schmitz B., Tassinari M., and Peucker-Ehrenbrink B. (2001) A rain of ordinary chondrite meteorites in the early Ordovician. *Earth Planet. Sci. Lett., 194,* 1–15.

Schmitz B., Häggström T., and Tassinari M. (2003) Sediment-dispersed extraterrestrial chromite traces a major asteroid disruption event. *Science, 300,* 961–964.

Schultz L. and Weber H. W. (1996) Noble gases and H chondrite meteoroid streams: No confirmation. *J. Geophys. Res., 101,* 21177–21181.

Schultz L., Weber W., and Begemann F. (1991) Noble gases in H chondrites and potential differences between Antarctic and non-Antarctic meteorites. *Geochim. Cosmochim. Acta, 55,* 59–66.

Schutt J., Schultz L., Zinner E., and Zolensky M. (1986) Search for meteorites in the Allan Hills region, 1985–1986. *Antarct. J., 21,* 82–83.

Sekanina Z. and Southworth R. B. (1975) *Physical and Dynamical Studies of Meteors: Meteor Fragmentation and Stream-Distribution Studies.* NASA CR-2615, U.S. Government Printing Office, Washington, DC.

Southworth R. B. and Sekanina Z. (1973) *Physical and Dynamical Studies of Meteors.* NASA CR-2316, U.S. Government Printing Office, Washington, DC.

Spurný P. (1997) Photographic monitoring of fireballs in central Europe. *Proc. SPIE, 3116,* 144–155.

Staubach P., Grün E., and Matney M. J. (2001) Synthesis of observations. In *Interplanetary Dust* (E. Grün et al., eds.), pp. 347–384. Springer-Verlag, Berlin.

Stuart J. S. and Binzel R. P. (2004) Bias-corrected population, size distribution, and impact hazard for the near-Earth objects, *Icarus, 170,* 295–311.

Taylor A. D. and Elford W. G. (1998) Meteoroid orbital element distributions at 1 AU deduced fromo the Harvard Radio Meteor Project observations. *Earth Planets Space, 50,* 569–575.

Tagliaferri E., Spalding R., Jacobs C., Worden S. P., and Erlich A. (1994) Detection of meteoroid impacts by optical sensors in Earth orbit. In *Hazards Due to Comets and Asteroids* (T. Gehrels, ed.), pp. 199–220. Univ. of Arizona, Tucson.

Thomas R. M. and Netherway D. J. (1989) Observations of meteors using an over-the-horizon radar. *Proc. Astron. Soc. Austral., 8,* 88–93.

Thomas P., Whitham P. S., and Wilford W. G. (1988) Response of high frequency radar to meteor backscatter. *J. Atmos. Terrestrial Phys., 50,* 703–724.

Trigo-Rodriguez J. M., Llorca J., Borovička J., and Fabregat J. (2004a) Chemical abundances from meteor spectra: I. Ratios of the main chemical elements. *Meteoritics & Planet. Sci., 38,* 1283–1294.

Trigo-Rodriguez J. M., Llorca J., and Fabregat J. (2004b) Chemical abundances from meteor spectra: II. Evidence for enlarged sodium abundances in meteoroids. *Mon. Not. R. Astron. Soc., 348,* 802–810.

Verniani F. (1973) An analysis of the physical parameters of 5759 faint radio meteors. *J. Geophys. Res., 78,* 8429–8462.

Wasson J. T. (1985) *Meteorites: Their Record of Early Solar-System History.* Freeman, New York.

Weissman P., Bottke W. F., and Levison H. F. (2002) Evolution of comets into asteroids. In *Asteroids III* (W. F. Bottke Jr. et al., eds.), pp. 669–686. Univ. of Arizona, Tucson.

Welten K. C. (1995) Exposure histories and terrestrial ages of Antarctic meteorites. Ph.D. thesis, Univ. of Utrecht. 150 pp.

Welten K. C., Alderliesten C., van der Borg K., and Lindner L. (1995) Cosmogenic beryllium-10 and aluminum-26 in Lewis Cliff meteorites. In *Workshop on Meteorites from Cold and Hot Deserts* (L. Schultz et al., eds.), pp. 65–70. LPI Tech. Rpt. 95-02, Lunar and Planetary Institute, Houston.

Welten K. C., Alderliesten C., van der Borg K., Lindner L., Loeken T. and Schultz L. (1997) Lewis Cliff 86360: An Antarctic L-chondrite with a terrestrial age of 2.35 million years. *Meteoritics & Planet. Sci., 32,* 775–780.

Werner S. C., Harris A. W. Neukum G., and Ivanov B. A. (2002) The near-earth asteroid size-frequency distribution: A snapshot of the lunar impactor size-frequency distribution. *Icarus, 156,* 287–290.

Wetherill G. W. (1986) Unexpected Antarctic chemistry. *Nature, 319,* 357–358.

Whillans I. M. and Cassidy W. A. (1983) Catch a falling star: Meteorites and old ice. *Science, 222,* 55–57.

Wieler R., Caffee M. W., and Nishiizumi K. (1995) Exposure and terrestrial ages of H chondrites from Frontier Mountain. In *Workshop on Meteorites from Cold and Hot Deserts* (L. Schultz et al., eds.), pp. 70–72. LPI Tech. Rpt. 95-02, Lunar and Planetary Institute, Houston.

Wlotzka F., Jull A. J. T., and Donahue D. J. (1995a) Carbon-14 terrestrial ages of meteorites from Acfer, Algeria. In *Workshop on Meteorites from Cold and Hot Deserts* (L. Schultz et al., eds.), pp. 72–73. LPI Tech. Rpt. 95-02, Lunar and Planetary Institute, Houston.

Wlotzka F., Jull A. J. T. and Donahue D. J. (1995b) Carbon-14 terrestrial ages of meteorites from Acfer, Algeria. In *Workshop on Meteorites from Cold and Hot Deserts* (L. Schultz et al., eds.), pp. 37–38. LPI Tech. Rpt. 95-02, Lunar and Planetary Institute, Houston.

Wolf S. F. and Lipschutz M. E. (1995a) Applying the bootstrap to Antarctic and non-Antarctic H-chondrite volatile-trace-element data. In *Workshop on Meteorites from Cold and Hot Deserts* (L. Schultz et al., eds.), pp. 73–75. LPI Tech. Rpt. 95-02, Lunar and Planetary Institute, Houston.

Wolf S. F. and Lipschutz M. E. (1995b) Yes, meteorite populations reaching the Earth change with time. In *Workshop on Meteorites from Cold and Hot Deserts* (L. Schultz et al., eds.), pp. 75–76. LPI Tech. Rpt. 95-02, Lunar and Planetary Institute, Houston.

Wolf S. F. and Lipschutz M. E. (1995c) Chemical studies of H chondrites — 7. Contents of Fe^{3+} and labile trace elements in Antarctic samples. *Meteoritics, 30,* 621–624.

Zolensky M. E. and Paces J. (1986) Alteration of tephra in glacial ice by "unfrozen water." *Geol. Soc. Am. Abstr. with Progr., 18,* 801.

Zolensky M. E., Wells G. L., and Rendell H. M. (1990) The accumulation rate of meteorite falls at the Earth's surface: The view from Roosevelt County, New Mexico. *Meteoritics, 25,* 11–17.

Zolensky M., Rendell H., Wilson I., and Wells G. (1992) The age of the meteorite recovery surfaces of Roosevelt County, New Mexico, USA. *Meteoritics, 27,* 460–462.

Zolensky M. E., Martinez R., and Martinez de los Rios E. (1995) New L chondrites from the Atacama Desert, Chile. *Meteoritics, 30,* 785–787.

Zolensky M. E., Abell P., and Tonui E. (2005) Metamorphosed CM and CI carbonaceous chondrites could be from the breakup of the same Earth-crossing asteroid (abstract). In *Lunar and Planetary Science XXXVI,* Abstract #2048. Lunar and Planetary Institute, Houston (CD-ROM).